Rising Temperatures, Rising Risks: A Three-Decade Analysis of Children's Heat Exposure in China (1990-2020)

Kai Feng, Marco M. Laghi, Jere R. Behrman, Emily Hannum, and Fan Wang*

March 19, 2024

Please click here for latest version of the paper.

Abstract

Children are more physically and physiologically vulnerable than adults to the ill effects of climatic and environmental shocks such as heat waves. There is a growing evidence linking extreme heat exposure to poorer developmental outcomes for children in domains ranging from education to health to long-term productivity. The frequency and intensity of heat waves are increasing as the earth's climate warms, but how these trends translate to changes in children's heat exposure is not well established. Changes in children's heat exposure are a joint function of changes in temperature and its geographic distribution and changes in the geographic distribution of the child population. Most studies that estimate the population burden of extreme heat 1) have focused on the total burden measured as person-time while overlooking within-population heterogeneities; 2) have not specifically focused on child populations; 3) have not explicitly attended to changing population distributions over time; 4) have relied on average temperature approaches without considering large hourly, daily and monthly temperature variations; and 5) have not estimated exposures at different, health-relevant temperature thresholds.

Using the case of China, the world's most populous country over the three recent decades studied, this paper estimates children's changing exposure to extreme high temperatures by linking county-level child population data to hourly Universal Thermal Climate Index (UTCI) data across two censuses spanning 30 years (1990-2020). We propose a convenient, low-data-demand framework for estimating the share of children at risk of extreme temperature exposures that 1) jointly considers temperature thresholds and the share of time exposed to such temperature thresholds, 2) jointly considers the geographical and temporal distributions of temperature and of children, and 3) allows for estimates for more and less extreme thresholds. Applying this framework to China, we find substantial increases in the average high-heat exposure for children and the share of children at risk and substantial regional heterogeneities. We also find that approximately half of the overall change in child high-heat exposure between 1990 and 2020 is driven by heat increases and the rest is driven by shifts in child population towards locations that have higher temperatures, illustrating the importance of paying attention to population distribution in addiion to temperature patterns.

Keywords: Extreme temperature, children

*Kai Feng: Department of Sociology and Population Studies Center, University of Pennsylvania, Philadelphia, Pennsylvania, USA; Marco M. Laghi: Department of Sociology, New York University, New York, NY, USA; Center for Applied Social and Economic Research, NYU Shanghai, Shanghai, China; Jere R. Behrman: Departments of Economics and Sociology and Population Studies Center, University of Pennsylvania, Philadelphia, Pennsylvania, USA; Emily Hannum: Department of Sociology and Population Studies Center, University of Pennsylvania, Philadelphia, Pennsylvania, USA; Fan Wang: Department of Economics, University of Houston, Houston, Texas, USA. This paper is supported by National Science Foundation Grants 1756738 and 2230615.

1 Introduction

Nearly half of the world's children live in countries identified by UNICEF's Children's Climate Risk Index (CCRI) as high-risk (UNICEF 2021), and children are highly physically and physiologically susceptible to climate-related disasters, hazards, and diseases. For example, children are highly vulnerable to daily thermo-regulatory stress and other health problems when exposed to extreme temperatures (UNICEF 2021; Xu et al. 2012). This growing evidence suggests that heat exposure affects children's short- and long-term development and welfare outcomes, from education to health to long-term productivity. At the same time though, most research on the distribution of climate risk has not considered special vulnerable groups like children. Connon and Dominelli (2022a, 2022b) are important exceptions with a key limitation. These UNICEF-partnered literature reviews together provide comprehensive new global evidence on how many children are currently exposed to a variety of climate and environmental hazards, shocks, and stresses, including heat waves, cyclones, river line flooding, coastal flooding, water scarcity, vector-borne diseases, air pollution, and lead pollution. These reviews inform UNICEF's CCRI (UNICEF 2021), which aggregates the different vulnerabilities and risks different children face and finds that approximately one billion children, nearly half of the world's children, live in "extremely high-risk countries" (p. 13). UNICEF (2022) goes into further detail and focuses on increasing durations of global heatwaves and projections for the future, using daily maximum temperatures to visualize global exposures for children using admittedly low-resolution data. These UNICEF reports thus contribute to understanding on a very aggregate level of children's climate risks and their heterogeneities across countries. However, UNICEF performs their analysis using aggregate geographic (i.e., nation-states) and time data (generally annual periods). This means that the results are not very fine-tuned at the micro level at which remedial or preventive policies must be developed and applied.

UNICEF's macro literature does not demonstrate distributional changes on the micro-level in children's heat exposure but still stands out in connecting concerns of heat exposure to children. Other globally focused works do not center this connection to children. As part of The Lancet's 2019 health and climate change report, Watts et al. (2019) lists heat exposure along with several other risk indicators for general and special populations but does not describe heat distribution within national contexts instead relying on international and national summary statistics. Further Watts et al. (2019) only considers the elderly as at-risk for heat waves

(p. 21), and when discussing child health primarily focuses on the outcomes of overall environmental risk rather than describing child-experienced exposures (pp. 11-12). Review literature like Ebi et al. (2021), Xu et al. (2012), and Xu et al. (2014) reinforce the common research trend of centering causal outcomes in other global heat literature on children without contextualizing distributions of exposure being experienced. Xu et al. (2012) and Xu et al. (2014) both explicitly use "mortality" and "morbidity" as keywords in their systematic reviews, finding results to suggest increased child mortality outcomes in high heat, and call for research that explores child heat exposure measurement. Ebi et al. (2021) reviews health risks and outcomes across the lifespan as a result of hot weather, but in discussing the exposure that leads to the outcomes refers to Byers et al. (2018) which uses mean temperature measures and days of heat exposure as well as grouping vulnerable populations solely through daily income.

A lack of focus on heat exposure distributions on children is not simply an issue of scale. We focus on the specific country context of China and find similar limitations. Much of the literature continues to center on causal impacts on children rather than observing existing exposure distributions. For China which is home to more than 253.38 million children ages 0-14 in the year 2020, this leaves a large research gap (National Bureau of Statistics of China 2021). The Chinese literature is broad and growing, showing cases of extreme heat exposure being linked to health outcomes including lower birth weights, more preterm birth, the common cold, hand, foot, and mouth diseases, and asthma (Guo et al. 2012; Liu et al. 2022; Lu et al. 2022; Lu et al. 2018; Ren et al. 2023; Xu et al. 2015), along with extreme temperatures being linked to poorer academic performance (Jiang et al. 2018; Wang et al. 2018). In short, research from China and elsewhere suggests that rising temperatures and associated increases in heat spells could have negative implications for children across a range of important life domains.

Still, China-centered studies have not yet rigorously established the extent to which heat exposure has been changing, let alone among children of which we have found no studies. One example of a line of research in China is not linked to population data and has shown an increase in the frequency of yearly high heat exposure days, with the highest intensities occurring outside of the North (Li and Zha 2020). Other studies estimate region-specific patterns alongside general population trends but still do not consider full distributions in doing so (Li and Zha 2020; Shi et al. 2021; Sun et al. 2020). Li and Zha (2020) tracks general population exposure trends over summers using daily maximum temperatures across China's different regions, finding the East to be the most exposed with rapid increases in population exposure

occurring in Central and Southern China. Shi et al. (2021) further supports this research in their findings on population exposure to diurnal heat-day trends across regions, which are found to increase further south in China. However, as another heat-day study (Sun et al. 2020) points out through their time-series analysis, while Southern and Eastern populations are experiencing higher and longer heatwaves, Northern populations may still be greatly affected due to a lack of physiological adaptation. Taking the existing research together, there is a need for considerations of special populations like children along with more nuanced data and methods that allow for both micro and macro understandings of changing distributions of heat exposure.

Our contribution to this literature is two-fold: we estimate the amount and intensity of heat stress that children have faced across China and offer a scale-able formula structured to use tabular census data linked with meteorological data. We link county-specific child population counts from Chinese censuses to hourly temperature data to estimate ambient heat-exposure risk for children between 1990 and 2020, incorporating geographic and temporal distributions of heat and the population of children. We propose and implement a framework for measuring the share of children at risk of extreme temperature exposures along with the average change of heat risk, jointly considering: 1) various temperature thresholds and 2) the share of time children are exposed to extreme heat using those temperature thresholds. In addition to attending to changes in the geographic distribution of the child population over time, this framework improves on many prior estimates of population burdens of heat exposure by capitalizing on temporally dis-aggregated data that allows consideration of significant heterogeneities in hourly variations in temperatures across space and allowing for estimation of exposure burdens at different temperature thresholds thought to be relevant to human health and functioning. Results from our exercise reveal substantial increases in average heat exposure for children and the share of children at risk. First, we show that the average child from 1990 to 2020 has experienced an increase in exposure to Moderate heat stress of 2.7 percentage points (pp). Second, we show that in 1990, 9.49% of children experienced Moderate or stronger heat stress for over 30% of their hours and that this figure increases by 10.02 pp in 2020. Third, we show that meteorology and population changes become mutually responsible for increasing heat stress among children. Finally, we show that there is substantial regional heterogeneity, with much of the national increase in child exposure to extreme heat attributable to population changes and movement of the Eastern region. Altogether, these results demon-

strate the value of our data framework which jointly utilizes temperature along with time and population distributions to estimate experienced risk for special populations.

2 Methods and Data

Methods. In this section, we summarize our framework and method for measuring child population at risk of heat exposure. Within a particular span of time in a region, our framework develops two statistics of temperature exposure risks building on two types of distributions and two types thresholds. The two distributions are the distribution of location-specific temperature and the distribution of population across locations conditional on population group (children). The two thresholds are temperature thresholds for extreme-temperature exposure and time thresholds for share of time exposed to extreme-temperature. The first risk statistics captures the risk of extreme temperature facing the average child, measured in units of share of time the average child is exposed to extreme temperature. The second risk statistics capture the distribution of risk among children, measured in units of the share of child population exposed to extreme temperatures for different durations of time.

In studies that consider population heat exposures, a prevalent metric for assessing heat exposure is the change in exposure in total person-time. Person-time exposure statistics are determined by both the population count and the duration of exposure to a specific risk factor over a given period in a particular location.[1] An aggregate statistic for a region or country is computed by summing person-time across locations within the region or country. While aggregate person-time serves as a valuable estimate for measuring the overall burden on a population, it has two limitations. First, when comparing exposures over time, aggregate person-time statistics will capture changes in aggregate population size over time in addition to changes in average heat exposure burdens. This situation makes results harder to interpret. For example, if the rate of population decline surpasses the rate of temperature increase, the resultant person-time estimates may diminish over time. Second, the person-time aggregate provides a single statistic of exposure for a region or country, overlooking the heterogeneities in ambient exposure changes across populations residing in locations with differing climatic change experiences. We propose a distributional approach to estimate the heterogeneities in changes of the percentages of children's time under heat stress.

1. The person-days of heat exposure in a place at time t can be computed, for example, by multiplying the days where the maximum temperature exceeds a threshold level with the total population residing in a place at time t.

In the closest related work, UNICEF (2022) estimates the aggregate number of children at risk of heat exposure based on the aggregate-population share of children. The closest related works focusing on all population groups generally provide different types of average aggregated statistics. Our framework is the first to jointly apply the double-distributions to compute the share of children (and population generally) at risk of the double-thresholds of exposure. We provide a detailed description of our methods in the appendix.

We implement our framework in the setting of China between 1990 and 2020. In this empirical application, we consider each span of time as one year, we approximate continuous ambient temperature exposure based on hourly estimates of temperature, and we approximate fine-grained measures of locations where the temperature gradient is non-zero with counties (3rd level administrative units) in China. For the temperature thresholds, we consider a range of thresholds but focus our analysis on key thresholds for extreme-heat commonly used in the literature. For time thresholds, we consider different shares of time during the course of the year exposed to temperatures above the thresholds considered. Our method is also straightforward to implement in other settings where tabular population data at relatively fine-grained level and location-specific climate data is available.

Data. In terms of climate data, we utilize the fifth generation of the European Centre for Medium-Range Weather Forecasts (ECMWF) atmospheric reanalyses of the global climate: the ERA5-HEAT dataset (Napoli 2020). ERA5-HEAT, a distinct advancement from its predecessors, offers hourly data on numerous climate variables with a spatial resolution of 0.25 degrees one of which we utilize is Universal Thermal Climate Index (UTCI). UTCI provides an integrative measure of the human-perceived equivalent temperature, taking into account factors like air temperature, humidity, wind speed, and radiant heat (Bröde et al. 2012; Jendritzky, Dear, and Havenith 2012; Jendritzky and Höppe 2017).

For population data, we utilize Chinese census data for the years 1990 and 2020 (All China Market Research Ltd 2022; Beijing Hua tong ren shi chang xin xi you xian ze ren gong si 2005a, 2005b; China Data Lab 2020). County-level population data, shapefiles, and microdata on demographic characteristics of age and gender were extracted and used to construct the population exposures by county.

For regional analysis, temperature and population data were sorted by province and assigned a region according to the four recognized economic regions of China (National Bureau

of Statistics of China 2011).

3 Results

Human perception of heat is influenced by various factors beyond just temperature. We adopt the Universal Thermal Climate Index that combines air temperature, humidity, wind speed, and radiation. It is widely used and provides a single value that represents the perceived thermal stress on the human body. When the UTCI is between 26°C and 32°C, it indicates moderate heat stress on the human body, signify warm conditions where individuals may start to feel uncomfortable, especially if engaging in physical activity. As the UTCI value increases, the level of thermal stress on the human body intensifies. UTCI between 32°C and 38°C indicate strong heat stress, whereas UTCI between 38°C and 36°C indicate very strong heat stress. The three-color background zone in Figure 1 reflects these stress categories.

Figure 1 depicts the percentage points change (Panel a) and percentage change (Panel b) in the average share of time in heat stress for children from 1990 to 2020 using three different time periods: all hours, daytime hours (6 a.m. - 10 p.m.), hot-month hours (April to September). Regardless of the focusing time periods, children's share of time in heat stress increased in China from 1990 to 2020 across all thresholds. The largest percentage point change (Figure 1 Panel a) occurs when considering only hours in hot months, followed by daytime hours, and then all annual hours. The percentage changes (Figure 1 Panel b) overlap more across the three time periods, except for daytime hours, which exhibit lower changes in the moderate heat stress category compared to the other two periods.

When all hours are considered, an average child in China experienced 20.09% of her total hours in 1990 at 26°C UTCI or above this threshold. By 2020, this percentage increased to 22.8%, representing a 2.7 percentage point (Figure 1 Panel a) and 13.5 % increase in annual average exposure duration (Figure 1 Panel b), which corresponds to an annual average increase of 238 hours of additional moderate or stronger heat stress exposure over 30 years.

While the change in percentage points in children's average share of time at risk of heat stress decreases with increasing minimal heat stress levels, the percent changes remain high until it declines after UTCI threshold of 35°C or above. For example, in 2020, the average duration of children's exposure to UTCI at or above 32°C increased by 1.1 percentage points, which is less than half compared to the change in the duration of exposure at 26°C or above.

However, this still reflects a 14.7% rise compared to the levels observed in 1990. These results also indicate that approximately 40% (calculated as $1 - \frac{2.7-1.1}{2.7} \approx 0.4$) of the increase can be attributed to the escalation in exposure to strong or above heat stress. Tables D.1 and D.2 in Appendix document the children's average share of time at risk of heat stress in 1990 and 2020 by UTCI thresholds using three different time periods defined above.

Increases in Share of Children at Risk of Heat Exposure. While the previous results focus on heat exposure for the average child in China, they do not provide information on how many children are increasingly at risk of heat exposure. In this section, given the distribution of heat and children across counties in China, we examine whether the *percentage* of children most affected by heat stress has also changed over time.

We compute the share of children at risk by considering jointly two thresholds of risks: a threshold for the level of heat stress exposure (intensity) and a threshold for the share of annual hours (duration) exposed to heat stress above a particular threshold. Figure 2 illustrates the combination of selected thresholds for the duration of time exposed to heat stress (from 4% to 36%) and the level of heat stress (from above 26°C to above 38°C). Tables D.3 and D.4 in the Appendix document the full extent of children surpassing thresholds of heat stress exposure by duration of time.

The exposure to at least some moderate heat stress is near universal to children in China. In 1990 (Figure 2 Panel a) and 2020 (Figure 2 Panel b), respectively, 97.2% and 97.7% of children experienced at least 4% of their hours, or over 2 weeks, in moderate or stronger heat stress (i.e. UTCI $\geqslant$ 26°C). As the duration of exposure to heat stress increased, the share of affected children decreased. However, the share of children enduring prolonged exposure to heat stress increased substantially from 1990 to 2020. In 1990, 6.7% of children experienced moderate or stronger heat stress for more than 36% of their time, or equivalently, for over 16 weeks. By 2020, this number rose to 13.7%, marking an increase of 7.0 percentage points (Figure 2 Panel c) or 106% (Table D.4 Panel b). In other words, the share of children experiencing *at least* moderate heat stress for *at least* 32% of their total hours in 2020 more than doubled compared to 1990.

A substantial increase in the share of children experiencing heat stress can be observed across various combinations of heat stress intensity and duration. For example, 11.2% (Figure 2 Panel a) of children had at least 12% of their total hours, or 6 weeks that are under strong heat

stress or above ($\geqslant$32°C). This number rose to 18.6% in 2020 (Figure 2 Panel b), representing a 7.4 percentage point (Figure 2 Panel c) or 66.3% increase (Table D.4 Panel b).

As the intensity of heat stress exposure increased, the share of children affected also declined. Yet, Figure 2 shows alarmingly fast increases in the share of children at risk to very strong heat stress. In particular, the share of children experiencing at least 4% of their total hours in at least very strong heat stress increased from 0.1% to 1.8%. While the share of children exposed to these extreme risk levels remains small, these increases represent approximately 1800-fold jumps in the share of children at these high exposure risk levels, approximately 45 million children.

Decomposing the Contributions of Changes in Climate and Population. Figure 3 depicts results from counterfactual decomposition analysis at the national level. This counterfactual analysis illustrates the extent to which changes in children's heat exposure over time can be attributed to shifts in the distribution of the child population, or to changes in the UTCI driven by meteorological changes. In this approach, we alter one distribution (either children's population or UTCI) while keeping the other constant, without modeling mechanisms of change. Unexplained changes are likely due to interactions between population and UTCI. In D.5, we also present decomposition results in Eastern region and Northeastern region.

Figure 3 demonstrates that the increase in average child's heat stress exposure from 1990 to 2020 results from both climate change and shifts in children's population distribution. For at least strong ($\geqslant$ 32 °C) and at least moderate heat ($\geqslant$ 26 °C) stress levels, child population distribution shifts account for 48% and 50% of the actual change, respectively. UTCI distribution shifts account for 42% and 40% of the actual changes, respectively.

While both population distribution change and climate change contribute to the rise in the average child's heat stress exposure, regional decomposition analysis shows varying impacts within regions (see D.5). Specifically, changes in population distribution account for about 1/3 of the exposure shifts in the Eastern region and less than 1/5 in the Northeastern region. This suggests that cross-regional shift in children distribution, such as migration to Eastern region or fertility decline in the Northeastern region, play a more significant role in explaining the population effect observed nationally.

Figure 3 also indicates that at higher UTCI thresholds, the influence of change in population distribution diminishes. Nationally, the contribution of population distribution shift in heat

stress exposure reduces with increasing thresholds, from 50% at UTCI above 26 °C to 39% at UTCI 36 °C. Similarly, the contributions of population distribution shift decline from 38% to 19% in Eastern region and from 16% to 5% in Northeastern region over the same UTCI thresholds. This suggests that the rise in more extreme heat exposures is primarily a result of climate change, rather than population shifts to already hotter areas in 1990.

Changes in Children's Heat Exposure Across Regions. Figure 4 (a) and (b) depict the average share of annual time at risk of heat stress for children in 1990 and 2020 respectively. Figure 4 (c) shows the percentage point (pp) change between 1990 and 2020. Children in both the Central and Eastern regions experience a high level of heat stress exposure. For instance, in 1990, an average child in the Eastern and Central regions would have faced at least moderate heat stress (above UTCI 26 °C) 23.6% and 23.4% of the time, and at least strong heat stress (above UTCI 26 °C) 8.4% and 9.3% of the time, respectively. The share of time exposed to at least moderate or at least strong heat stress in these two regions remained high in 2020 as shown in Figure 4 (b). The percentage point changes in the share of time at risk of heat exposure are notable across various UTCI thresholds in the Eastern region, with a 4.4 pp at above 26 °C and a 1.7 percentage point increase at 32 °C. In contrast, the changes in the share of time remain below 1 pp across UTCI thresholds (Figure 4 (c)). The comparison indicates that although children in both regions spend a significant amount of time exposed to heat, those in the Eastern region face a heightened challenge in adapting to heat stress owing to the rapid increase in exposure duration.

Compared to Eastern and Central regions, the Northeastern region had relatively low average child heat exposure in 1990. However, the children's share of annual time in Northeastern region experienced increases of 19% ($\geqslant$ 26 °C) and 36% ($\geqslant$ 29 °C) for average at least Moderate heat stress and 106% ($\geqslant$ 32 °C) and 457% ($\geqslant$ 35 °C) for at least Strong heat stress. In 2020, the average Northeastern region child experienced 8.9% and 2.4% of her time under at least Moderate ($\geqslant$ 26 °C) and at least strong ($\geqslant$ 32 °C) heat stress, which are still much lower than average exposure levels in Central and Eastern regions.

Table D.7 and D.8 in Appendix provide additional results on changes in children's shares of annual time exposed to heat stress at the province level. In 2020, Hainan (Eastern), Guangdong (Eastern), Guangxi (Western), Jiangxi (Central), and Fujian (Eastern) are generally ranked from top 1 to 5 in terms of average share of child time exposed to heat across all UTCI thresholds.

Specifically, in 2020, children in Hainan, Guangdong, Guangxi, Jiangxi and Fujian had on average 19.2%, 15.2%, 13.2%, 12.8%, and 11.8% share of time exposed to at least Strong heat stress (UTCI $\geqslant$ 32 °C), which represented respective increases of 17%, 20%, 8%, 16%, and 54% in share of time exposed compared to 1990.

While Northeastern and Eastern provinces (excluding Jiangsu) experienced substantial increases in heat exposure, provinces in Central and Western regions experienced limited exposure increases and reductions. In particular, Central China's provinces of Hubei and Anhui and Western China's provinces of Shaanxi and Sichuan generally experienced reductions in average child heat exposures across UTCI thresholds. Additionally, children in Qinghai and Xizang (Tibet) in the Western region continue to have generally no exposure to at least Moderate heat stress.

4 Discussion and Conclusion

In this paper, we combined county-level census population data on child distribution from 1990 and 2020 with temperature data to study changes in ambient heat exposure facing children over three decades. We find substantial increases in the average heat exposure for children and the share of children at risk and substantial regional heterogeneity. Interestingly, we find that half of the overall changes in high child heat exposure are driven by heat increases and the rest is driven by shifts in child population towards hotter locations.

In our first result, we found that in 1990, an ***average*** child in China experienced moderate or stronger heat stress (UTCI $\geqslant$ 26°C and above) for 20.09 % of their hours. By 2020, this percentage had increased by 2.7 percentage points (pp) (Figure 1). In our second result, we found that in 1990, 9.49 % of children experienced moderate or stronger heat stress for over 30% of their hours. By 2020, this figure had risen to 19.51%, marking an increase of 10.02 pp (Figure 2).

For our third result, counterfactual decomposition analyses reveal that the effects of escalating temperatures and a growing child population in the heat-affected regions contribute equally to the overall increase in heat exposure among children (Figure 3). For the fourth result, the substantial increase in children's exposure to heat stress in Eastern China, the nation's most economically developed and densely populated region, is a primary driver behind the overall surge observed at the national level (Figure 4).

We implicitly assume uniform sensitivity and adaptability to heat stress among all individuals, overlooking the potential adaptability of those residing in warmer regions. Our definition of heat exposure is simplified, and future research could adopt the same methodology with different definitions of heat stress. For instance, exploring heat wave episodes rather than focusing solely on single hours above the heat stress threshold could provide a more comprehensive understanding. Additionally, while our focus is on total hours, it's important to acknowledge that children may tend to stay indoors with air conditioners during heat waves, and the ability to withstand heat stress may vary by socioeconomic status. Lastly, despite utilizing county-level data, a more granular measure may better capture heat stress even using our same framework, particularly in urban areas where factors like the heat island effect come into play.

References

All China Market Research Ltd. 2022. *2020 China County Population Census Data with GIS Maps.*

Beijing Hua tong ren shi chang xin xi you xian ze ren gong si. 2005a. *1990 County Boundaries of China with Population Census Data, Part 1 & 2. [Shapefile].* https://geo.nyu.edu/catalog/nyu-2451-34775.

———. 2005b. *China Historical 2000 County Population Census Data.* https://geo.nyu.edu/catalog/harvard-ch-census2000.

Bröde, Peter, Dusan Fiala, Krzysztof Błażejczyk, Ingvar Holmér, Gerd Jendritzky, Bernhard Kampmann, Birger Tinz, et al. 2012. "Deriving the Operational Procedure for the Universal Thermal Climate Index (UTCI)." *International Journal of Biometeorology* 56, no. 3 (May 1, 2012): 481–494. https://doi.org/10.1007/s00484-011-0454-1.

Byers, Edward, Matthew Gidden, David Leclère, Juraj Balkovic, Peter Burek, Kristie Ebi, Peter Greve, et al. 2018. "Global Exposure and Vulnerability to Multi-Sector Development and Climate Change Hotspots." *Environmental Research Letters* 13, no. 5 (May 1, 2018): 055012. https://doi.org/10.1088/1748-9326/aabf45.

China Data Lab. 2020. *China County Map with 2000-201o Population Census Data.* In collaboration with China Data Lab. https://doi.org/10.7910/DVN/VKGEBX.

Connon, Irena, and Lena Dominelli. 2022a. *Rapid Literature Review: Children and Heat Waves.* UNICEF Children's Climate Change Risk Index (CCRI). Data for Children Collaborative, September. https://www.dataforchildrencollaborative.com/outputs/rapidreview-heatwaves-tmha3.

———. 2022b. *Systematic Review of the Literature: Findings, Outcomes and Policy Recommendations.* UNICEF Children's Climate Change Risk Index (CCRI). Data for Children Collabortive and UNICEF, April. http://dspace.stir.ac.uk/handle/1893/34193.

Dong, Diwen, Hui Tao, and Zengxin Zhang. 2023. "Historic Evolution of Population Exposure to Heatwaves in Xinjiang Uygur Autonomous Region, China." *Scientific Reports* 13, no. 1 (May 6, 2023): 7401. https://doi.org/10.1038/s41598-023-34123-w.

Ebi, Kristie L, Anthony Capon, Peter Berry, Carolyn Broderick, Richard De Dear, George Havenith, Yasushi Honda, et al. 2021. "Hot Weather and Heat Extremes: Health Risks." *The Lancet* 398, no. 10301 (August): 698–708. https://doi.org/10.1016/S0140-6736(21)01208-3.

Feng, Yao, Wenbin Liu, Hong Wang, Fa Liu, and Fubao Sun. 2023. "Multifaceted Characteristics of Summer Heat and Affected Population Across China Under Climate Change." *Climate Dynamics* 61, no. 5 (September): 2173–2187. https://doi.org/10.1007/s00382-023-06671-4.

Guo, Yuming, Fan Jiang, Li Peng, Jun Zhang, Fuhai Geng, Jianming Xu, Canming Zhen, et al. 2012. "The Association Between Cold Spells and Pediatric Outpatient Visits for Asthma in Shanghai, China." *PLOS ONE* 7, no. 7 (July 25, 2012): e42232. https://doi.org/10.1371/journal.pone.0042232.

Hu, Lisuo, Gang Huang, and Xia Qu. 2017. "Spatial and Temporal Features of Summer Extreme Temperature Over China During 1960–2013." *Theoretical and Applied Climatology* 128, no. 3 (May): 821–833. https://doi.org/10.1007/s00704-016-1741-x.

Jendritzky, Gerd, Richard de Dear, and George Havenith. 2012. "UTCI—Why Another Thermal Index?" *International Journal of Biometeorology* 56, no. 3 (May 1, 2012): 421–428. https://doi.org/10.1007/s00484-011-0513-7.

Jendritzky, Gerd, and Peter Höppe. 2017. "The UTCI and the ISB." *International Journal of Biometeorology* 61, no. 1 (September 1, 2017): 23–27. https://doi.org/10.1007/s00484-017-1390-5.

Jiang, Jing, Dengjia Wang, Yanfeng Liu, Yanchao Xu, and Jiaping Liu. 2018. "A Study on Pupils' Learning Performance and Thermal Comfort of Primary Schools in China." *Building and*

Environment 134 (April 15, 2018): 102–113. https://doi.org/10.1016/j.buildenv.2018.02.036.

Li, Long, and Yong Zha. 2020. "Population Exposure to Extreme Heat in China: Frequency, Intensity, Duration and Temporal Trends." *Sustainable Cities and Society* 60 (September): 102282. https://doi.org/10.1016/j.scs.2020.102282.

Liu, Xiaoying, Jere Behrman, Emily Hannum, Fan Wang, and Qingguo Zhao. 2022. "Same Environment, Stratified Impacts? Air Pollution, Extreme Temperatures, and Birth Weight in South China." *Social Science Research* 105 (July 1, 2022): 102691. https://doi.org/10.1016/j.ssresearch.2021.102691.

Lu, Chan, Zijing Liu, Hongsen Liao, Wenhui Yang, Qin Liu, Qin Li, and Qihong Deng. 2022. "Interaction of Exposure to Outdoor Air Pollution and Temperature During Pregnancy on Childhood Asthma: Identifying Specific Windows of Susceptibility." *Building and Environment* 225 (November 1, 2022): 109676. https://doi.org/10.1016/j.buildenv.2022.109676.

Lu, Chan, Yufeng Miao, Ji Zeng, Wei Jiang, Yong-Ming Shen, and Qihong Deng. 2018. "Prenatal Exposure to Ambient Temperature Variation Increases the Risk of Common Cold in Children." *Ecotoxicology and Environmental Safety* 154 (June): 221–227. https://doi.org/10.1016/j.ecoenv.2018.02.044.

Luo, Ming, and Ngar-Cheung Lau. 2019. "Characteristics of Summer Heat Stress in China During 1979–2014: Climatology and Long-Term Trends." *Climate Dynamics* 53, no. 9 (November): 5375–5388. https://doi.org/10.1007/s00382-019-04871-5.

Napoli, Claudia Di. 2020. *Thermal Comfort Indices Derived from ERA5 Reanalysis.* https://doi.org/10.24381/CDS.553B7518.

National Bureau of Statistics of China. 2011. *[Method of Dividing the East, West, Central and Northeast Regions].* Beijing: State Council of China, June 13, 2011. https://web.archive.org/web/20190323041213/http://www.stats.gov.cn/ztjc/zthd/sjtjr/dejtjkfr/tjkp/201106/t20110613_71947.htm.

———. 2021. *Main Data of the Seventh National Population Census.* Beijing: State Council of China, May 11, 2021. https://www.unicef.cn/en/media/24511/file/What%20the%202020%20Census%20Can%20Tell%20Us%20About%20Children%20in%20China%20Facts%20and%20Figures.pdf.

Ren, Meng, Chunying Zhang, Jiangli Di, Huiqi Chen, Aiqun Huang, John S. Ji, Wannian Liang, et al. 2023. "Exploration of the Preterm Birth Risk-Related Heat Event Thresholds for Pregnant Women: A Population-Based Cohort Study in China." *The Lancet Regional Health - Western Pacific* 37 (August): 100785. https://doi.org/10.1016/j.lanwpc.2023.100785.

Shi, Ying, Zhenyu Han, Ying Xu, and Chan Xiao. 2021. "Impacts of Climate Change on Heating and Cooling Degree-hours Over China." *International Journal of Climatology* 41, no. 3 (March 15, 2021): 1571–1583. https://doi.org/10.1002/joc.6889.

Sun, Zhaobin, Xiaoling Zhang, Ziming Li, Yinglin Liang, Xingqin An, Yuxin Zhao, Shiguang Miao, et al. 2024. "Heat Exposure Assessment Based on High-Resolution Spatio-Temporal Data of Population Dynamics and Temperature Variations." *Journal of Environmental Management* 349 (January): 119576. https://doi.org/10.1016/j.jenvman.2023.119576.

Sun, Zhiying, Chen Chen, Meilin Yan, Wanying Shi, Jiaonan Wang, Jie Ban, Qinghua Sun, et al. 2020. "Heat Wave Characteristics, Mortality and Effect Modification by Temperature Zones: A Time-Series Study in 130 Counties of China." *International Journal of Epidemiology* 49 (6): 1813–1822. https://doi.org/10.1093/ije/dyaa104.

UNICEF. 2021. "The Climate Crisis is a Child Rights Crisis," August 20, 2021. https://www.unicef.org/reports/climate-crisis-child-rights-crisis.

UNICEF. 2022. *The Coldest Year of the Rest of Their Lives: Protecting Children Form the Escalating Impacts of Heatwaves.* New York: UNICEF. https://www.unicef.org/media/129506/file/UNICEF-coldest-year-heatwaves-and-children-EN.pdf.

Wang, Dengjia, Yanchao Xu, Yanfeng Liu, Yingying Wang, Jing Jiang, Xiaowen Wang, and Jiaping Liu. 2018. "Experimental Investigation of the Effect of Indoor Air Temperature on Students' Learning Performance Under the Summer Conditions in China." *Building and Environment* 140 (August): 140–152. https://doi.org/10.1016/j.buildenv.2018.05.022.

Wang, Dongqian, and Ying Sun. 2021. "Long-Term Changes in Summer Extreme Wet Bulb Globe Temperature Over China." *Journal of Meteorological Research* 35, no. 6 (December): 975–986. https://doi.org/10.1007/s13351-021-1080-4.

Watts, Nick, Markus Amann, Nigel Arnell, Sonja Ayeb-Karlsson, Kristine Belesova, Maxwell Boykoff, Peter Byass, et al. 2019. "The 2019 Report of the Lancet Countdown on Health and Climate Change: Ensuring That the Health of a Child Born Today is Not Defined by a Changing Climate." *The Lancet* 394, no. 10211 (November): 1836–1878. https://doi.org/10.1016/S0140-6736(19)32596-6.

Wu, Jia, Xuejie Gao, Filippo Giorgi, and Deliang Chen. 2017. "Changes of Effective Temperature and Cold/hot Days in Late Decades Over China Based on a High Resolution Gridded Observation Dataset." *International Journal of Climatology* 37 (S1): 788–800. https://doi.org/10.1002/joc.5038.

Xu, Meimei, Weiwei Yu, Shilu Tong, Lei Jia, Fengchao Liang, and Xiaochuan Pan. 2015. "Non-Linear Association Between Exposure to Ambient Temperature and Children's Hand-Foot-and-Mouth Disease in Beijing, China." Edited by Qinghua Sun. *PLOS ONE* 10, no. 5 (May 26, 2015): e0126171. https://doi.org/10.1371/journal.pone.0126171.

Xu, Zhiwei, Ruth A. Etzel, Hong Su, Cunrui Huang, Yuming Guo, and Shilu Tong. 2012. "Impact of Ambient Temperature on Children's Health: A Systematic Review." *Environmental Research* 117 (August): 120–131. https://doi.org/10.1016/j.envres.2012.07.002.

Xu, Zhiwei, Perry E. Sheffield, Hong Su, Xiaoyu Wang, Yan Bi, and Shilu Tong. 2014. "The Impact of Heat Waves on Children's Health: A Systematic Review." *International Journal of Biometeorology* 58, no. 2 (March): 239–247. https://doi.org/10.1007/s00484-013-0655-x.

Yan, Yechao, Dandan Wang, Shuping Yue, and John Qu. 2019. "Trends in Summer Air Temperature and Vapor Pressure and Their Impacts on Thermal Comfort in China." *Theoretical and Applied Climatology* 138, no. 3 (November): 1445–1456. https://doi.org/10.1007/s00704-019-02909-6.

You, Qinglong, Zhihong Jiang, Lei Kong, Zhiwei Wu, Yutao Bao, Shichang Kang, and Nick Pepin. 2017. "A Comparison of Heat Wave Climatologies and Trends in China Based on Multiple Definitions." *Climate Dynamics* 48, no. 11 (June): 3975–3989. https://doi.org/10.1007/s00382-016-3315-0.

Zhou, Botao, Ying Xu, Jia Wu, Siyan Dong, and Ying Shi. 2016. "Changes in Temperature and Precipitation Extreme Indices Over China: Analysis of a High-resolution Grid Dataset." *International Journal of Climatology* 36, no. 3 (March): 1051–1066. https://doi.org/10.1002/joc.4400.

Figure 1: Change in Average Share of Time at or above UTCI Thresholds for Children 1990-2020

(a) Changes between 1990 and 2020 in percentage points

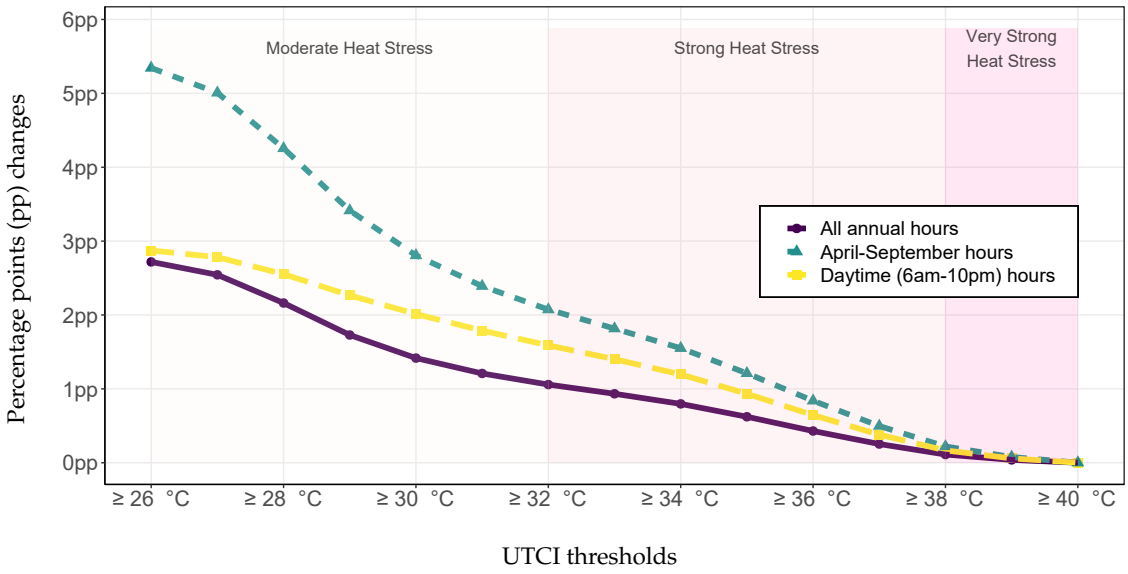

(b) Changes between 1990 and 2020 in percentage

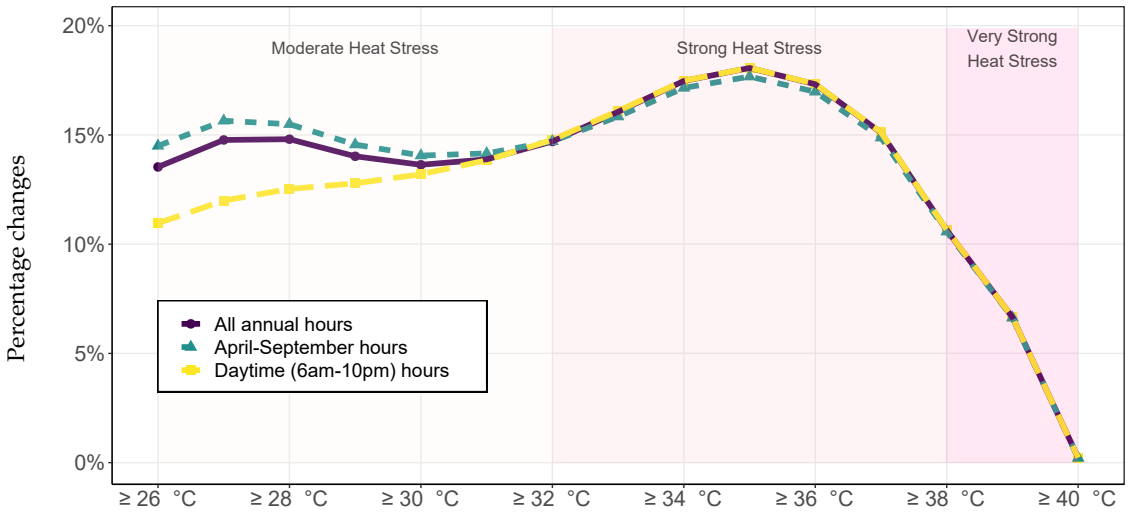

Notes: The y-axis denotes the percentage increase in hourly heat exposure for an average child in China from 1990 to 2020. The size of the circle represents the percentage point increase in hour heat exposure for an average child in China from 1990 to 2010. The circle in red shows the results when all hours are included, whereas the circle in blue shows the results when day-time hours are included. Table D.1 in Appendix documents the exact values.

Figure 2: Share of Children at Risk of Heat Stress, 1990 to 2020

(a) 1990

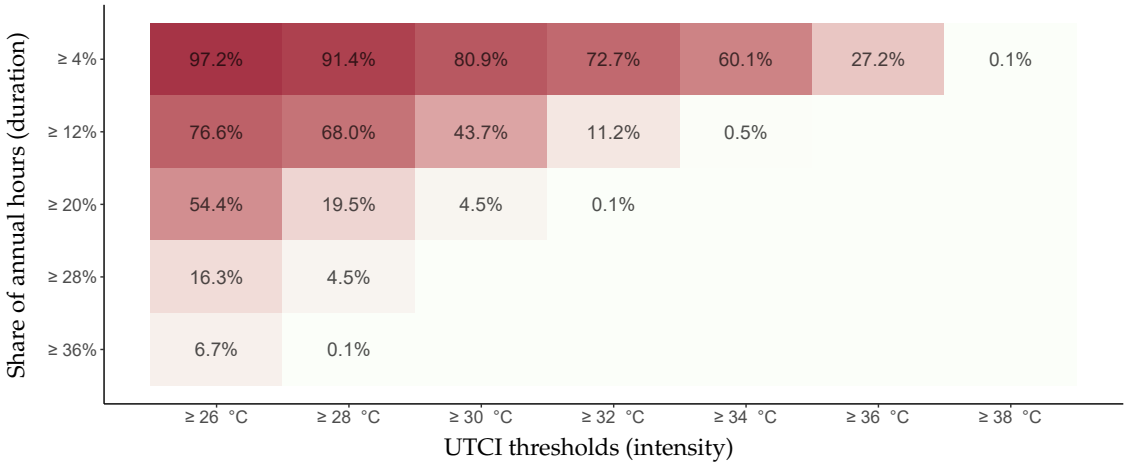

(b) 2020

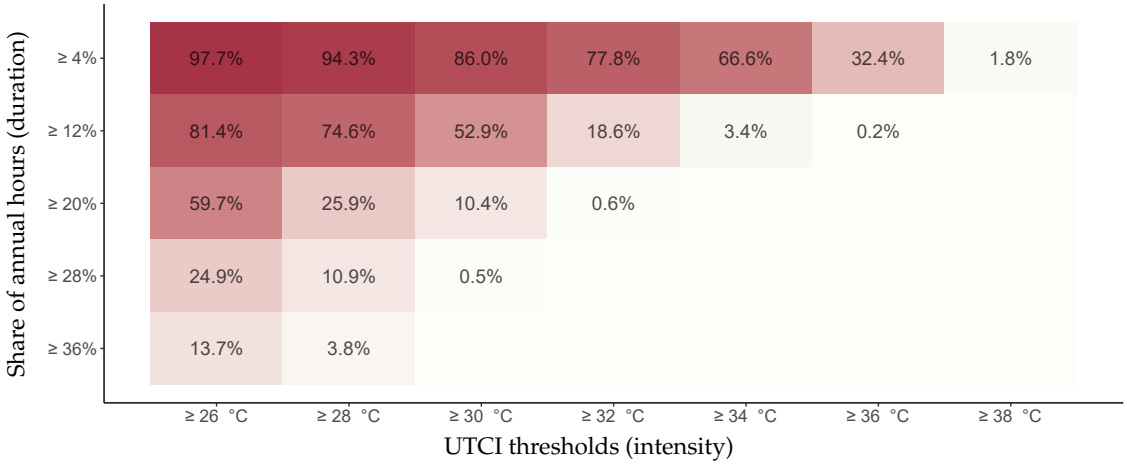

(c) Changes between 1990 and 2020 in percentage points

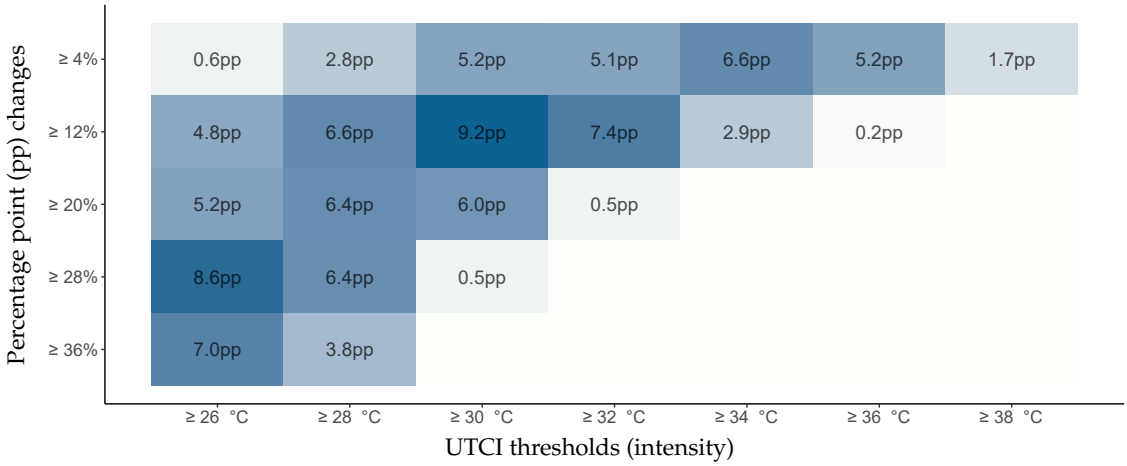

Notes: The y-axis denotes the percentage increase in hourly heat exposure for an average child in China from 1990 to 2020. The size of the circle represents the percentage point increase in hour heat exposure for an average child in China from 1990 to 2010. The circle in red shows the results when all hours are included, whereas the circle in blue shows the results when daytime hours are included. Table D.1 in Appendix documents the exact values.

Figure 3: Decomposed Change in Average Share of Time Children at Risk of Heat Stress

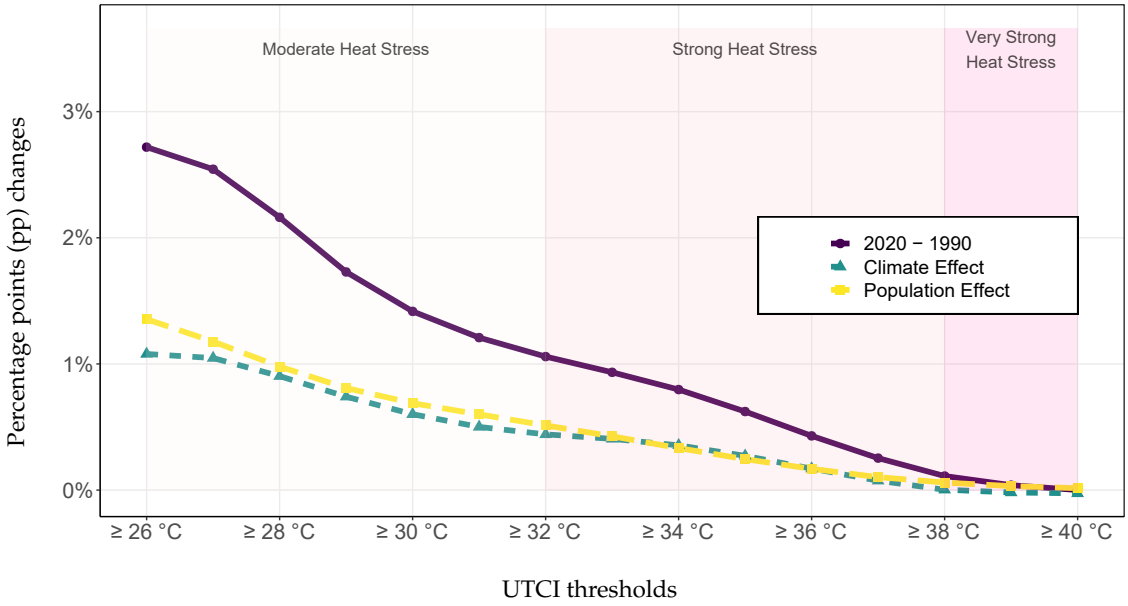

Notes: The purple solid line represents the percentage point difference in average share of time at risk of exposure to heat stress for children ages 0 to 14 between 1990 and 2020 (the year of 1990 as reference). In the first counterfactual decomposition, we use children population distribution in 1990 with the observed temperature in 2020. The green short-dash line represents the percentage difference between the decomposition results with the baseline (climte effect). In the second counterfactual decomposition, we use children population distribution in 2020 with the observed temperature in 1990. The yellow long-dash line represents the percentage difference between the decomposition results with the baseline (population effect).

Figure 4: Regional Average Share of Time at Risk of Heat Stress for Children, 1990 to 2020

(a) 1990

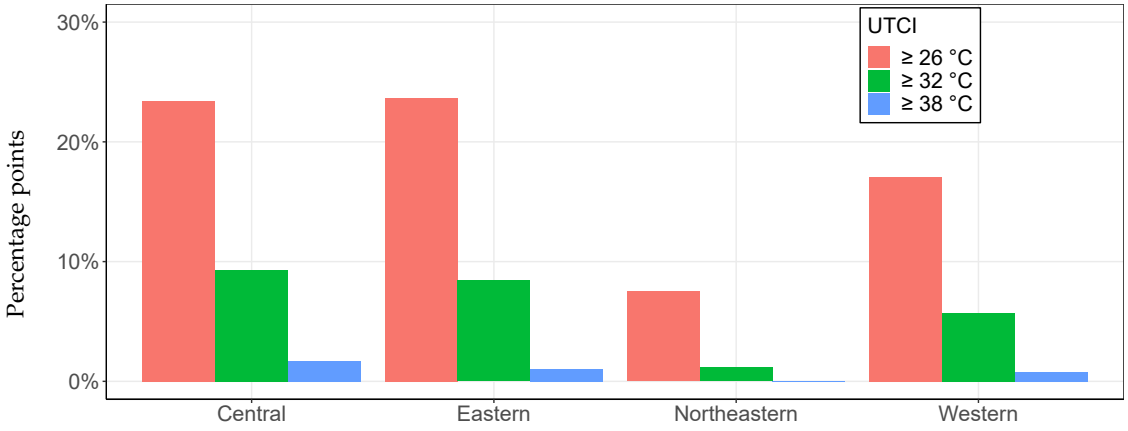

(b) 2020

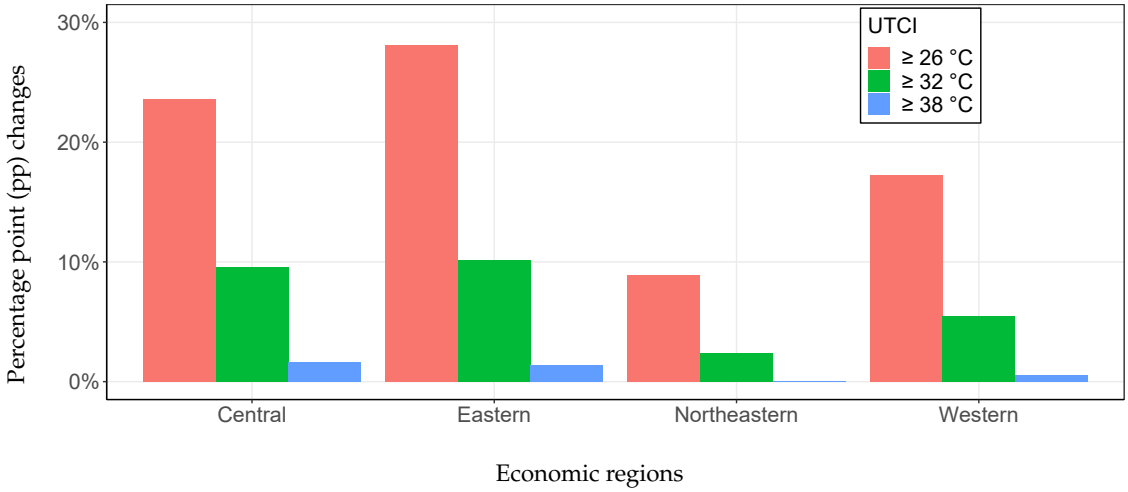

(c) Changes between 1990 and 2020 in percentage points

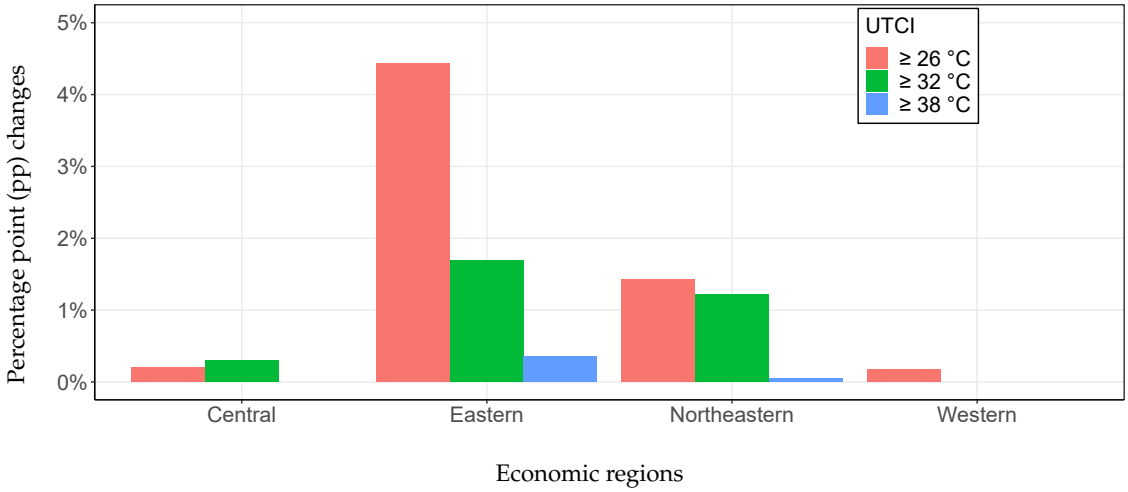

Notes: The y-axis depicts the percentage point difference from 2020 and 1990 heat exposure for children ages 0-14. We display these differences across the four economic regions of China and across different thresholds of heat exposure (moderate, strong, and very strong).

ONLINE APPENDIX

Rising Temperatures, Rising Risks: A Three-Decade Analysis of Children's Heat Exposure in China (1990-2020)

Kai Feng, Marco M. Laghi, Jere R. Behrman, Emily Hannum, and Fan Wang

A Method—Population, Time, and Temperature Exposure

A.1 Population, Time, and Temperature Exposure

We now formalize our temperature-exposure analysis framework across time and space. Specifically, let $c_l(t)$ be the UTCI temperature experienced by an individual at a moment in time t at a location l. Between period $\underline{t}$ and $\underline{t}+\tau$, the share of time that individuals at location l experience temperature $c_l(t)$ over threshold c^* is, $s_l(c^*, \underline{t}, \tau)$:

$$s_l(c^*, \underline{t}, \tau) = \frac{1}{\tau}\int_{\underline{t}}^{\underline{t}+\tau} \mathbf{1}\{c_l(t) > c^*\}\, dt\ . \tag{1}$$

Additionally, let $P_{\underline{t}\leqslant t<\underline{t}+\tau}(l|m)$ be the share of population for socio-demographic group m in a location l, among L locations in total between time $\underline{t}$ and $\underline{t}+\tau$ where: $\sum_{l=1}^{L} P_{\underline{t}\leqslant t<\underline{t}+\tau}(l|m) = 1$. Meaning that the population m at location l is experiencing exposure.

We compute two key sets of statistics. First, we compute $S_m(c^*, \underline{t}, \tau)$, which is for a particular interval of time, the average share of time individuals of a socio-demographic group m are exposed to temperature over threshold c^*:

$$S_m(c^*, \underline{t}, \tau) = \sum_{l=1}^{L} P_{\underline{t}\leqslant t<\underline{t}+\tau}(l|m)\cdot s_l(c^*, \underline{t}, \tau)\,. \tag{2}$$

Since $S_m(c^*, t, \tau)$ is a share of time, it is between 0 and 1. In particular, $\lim_{c^*\to\infty} S_m(c^*, t, \tau) = 0$ and $\lim_{c^*\to-\infty} S_m(c^*, t, \tau) = 1$. A key aggregate statistic for how temperature exposure shifts between period t' and t is the following difference:

$$\Delta S_{m,t',t}(c^*, \tau) = S_m\left(c^*, t', \tau\right) - S_m(c^*, t, \tau)\,. \tag{3}$$

$\Delta S_{m,t',t}(c^*, \tau)$ is the population-weighted average increase in the share of time exposed to the potential key temperature threshold c^* between time t and t' for population group m. $\Delta S_{m,t',t}(c^*, \tau)$ shifts due to both shifts in the population distribution as well as the distribu-

tion of temperature between t and t', thus taking into account population and meteorological change.

Second, we compute the share of individuals at risk, based on a joint consideration of the relevant temperature threshold that might be considered risky for human development, and the share of time exposed to such temperature that would put individuals at risk of non-transitory impacts. Our objective here is not to provide what these thresholds should specifically be but to consider, for the first time, these two joint dimensions of risks in computing population-demographic-related exposure statistics. Specifically, let $s^*(\tau)$ be a particular share-of-time threshold within span of time τ above a specific temperature risk threshold. In our analysis, we use an $s^*(\tau)$ of 0.10; 0.20; and 0.30 as shares of time above each UTCI temperature between 26 and 32. We define the m-, c^*-, and s^*-specific at risk measure $\mathcal{R}_m(c^*, s^*, t, \tau)$ between time t and $t+\tau$ as:

$$\mathcal{R}_m(c^*, s^*, \underline{t}, \tau) = \sum_{l=1}^{L} P_{\underline{t} \leqslant t < \underline{t}+\tau}(l|m) \cdot \mathbf{1}\{s_l(c^*, \underline{t}, \tau) > s^*(\tau)\}. \tag{4}$$

By construction, $\mathcal{R}_m(c^*, s^* = 0, t, \tau) \leqslant 1$ and $\mathcal{R}_m(c^*, s^* = 1, t, \tau) = 0$. Additionally, the share of individuals experiencing greater than s^* share of time over c^* threshold converges to 0 as c^* increases: $\lim_{c^* \to \infty} \mathcal{R}_m(c^*, s^*, t, \tau) = 0$.

For the socio-demographic group indexed by m, given temperature threshold c^* and share of time threshold s^*, the percentage increase over time in the share of individuals from this group at risk of excess heat exposure is:

$$\Delta\mathcal{R}_{m,t',t}(c^*, s^*, \tau) = \mathcal{R}_m\left(c^*, s^*, t', \tau\right) - \mathcal{R}_m(c^*, s^*, t, \tau). \tag{5}$$

In our empirical application t is 1990 and, t' is 2020, τ is one calendar year, and m is children between age 0 to 14. Additionally, we approximate continuous time with hourly measurements. As an example, $\Delta\mathcal{R}_{\text{children},2020,1990}$ with $c^* = 28$ and $s^* = 0.1$ provides the change in the percentage points of children exposed to temperature over 28 degrees for greater than 10 percent of their time during a year.

One important aspect of our framework is that computing $\mathcal{R}_m(c^*, s^*, t, \tau)$ and $\Delta\mathcal{R}_{m,t',t}(c^*, s^*, \tau)$ do not require the use of harmonized geographic data overtime. This is often a constraint in the analysis of temperature changes over time, due to shifting boundaries of administrative boundaries, especially across large spans of time. In our analysis, the unit of interest is m, the

socio-demographic group; at times t and t', thus the geographical boundaries can shift.

A.2 Life-cycle Share of Heat Time (Comment out later, this is not applicable for this paper, but applicable in settings with life-cycle history)

Define the temperature exposure for an indivdual child along life cycle Below we define the share of time exposured to temperature over $c*$ during the time segment j.

$$s_{l_j}(c^*, \underline{t}_j, \tau_j) = \frac{1}{\tau_j} \int_{\underline{t}_j}^{\underline{t}_j + \tau_j} \mathbf{1}\{c_{l_j}(t) > c^*\} dt \,. \tag{6}$$

During a child's life-cycle, there are J segments, where $j = 1$ is the conception period, then $j = 2$ is from birth to first move, etc. The total time since conception is T:

$$T = \sum_{j=1}^{J} \tau_j. \tag{7}$$

Accumulating up across the J life-cycle components, we compute the total share of time a child experiences in entire life cycle with J segments of exposure over c^* threshold:

$$s\left(c^*, \left\{\underline{t}_j, \tau_j, l_j\right\}_{j=1}^{J}\right) = \sum_{j=1}^{J} \left(\frac{\tau_j}{T} \cdot s_{l_j}(c^*, \underline{t}_j, \tau_j)\right) \tag{8}$$

The $s(\cdot)$ function is child-specific. So we can compute this, and look at the distribution of heat exposure for each child, and then we can consider the aggregate distribution across all children.

Average exposure across children Now we add an individual subscript to the previously derived share of time formula

$$s\left(c^*, \left\{\underline{t}_{i,j}, \tau_{i,j}, l_{i,j}\right\}_{j=1}^{J}\right) \tag{9}$$

Let there there N children, and $\widehat{J}$ be the subset of time segments to be considered. the average exposure average the life cycle of all children is

$$\mathcal{S}\left(c^*, \widehat{J}\right) = \frac{1}{N} \cdot \sum_{i=1}^{N} s\left(c^*, \left\{\underline{t}_{i,j}, \tau_{i,j}, l_{i,j}\right\}_{j \in \widehat{J}}\right) \tag{10}$$

Average exposure across children from different socio-demographic and location and other groupings Let $\widehat{I}_m$ be the set of children in group m, and let M_m be the number of children in this group, The average share of time children from demographic group m, are exposure to heat during lifecycle segments $\widehat{J}$ is now:

$$\mathcal{S}\left(c^*, \widehat{J}, \widehat{I}_m\right) = \frac{1}{M_m} \cdot \sum_{i \in \widehat{I}_m} s\left(c^*, \left\{\underline{t}_{i,j}, \tau_{i,j}, l_{i,j}\right\}_{j \in \widehat{J}}\right) \tag{11}$$

B Data

B.1 ERA5 Data Details

ERA5-HEAT, produced by the European Centre for Medium-Range Weather Forecasts (ECMWF), represents the fifth generation of atmospheric reanalyses of global climate (Napoli 2020). Covering the period from 1979 to the present, ERA5-HEAT comprises hourly gridded maps of the Universal Thermal Climate Index (UTCI) at 0.25° × 0.25° spatial resolution. The dataset is publicly accessible through the Copernicus Climate Change Service's Climate Data Store (CDS).

For standard geo-based analysis over time, a key stumbling block is harmonizing location boundaries that may change over time. This is normally difficult to deal with when we have county-level boundaries, as Chinese administrative names and boundaries have changed substantially over 30 years. Luckily, we are not necessarily trying to compare a county to its own borders across 30 years, instead, we compare similarly fine and consistent measures of population and temperature distribution across time that in this case match well with county boundaries. Another option might be to proceed is via the use of prefecture data in 1990 and county data in 2020, but that might not be as appropriate or easily interpretable.

As described by Bröde et al. (2012), Jendritzky, Dear, and Havenith (2012), and Jendritzky and Höppe (2017), the UTCI is a widely used index to assess the human-perceived environment based on atmospheric conditions, integrating atmospheric parameters like temperature, humidity, wind speed, and solar radiation. UTCI is expressed in degrees Celsius (°C), and it provides a measure of how cold or hot people might feel under prevailing environmental conditions. The index categorizes thermal stress into different classes with corresponding thresholds, which are as follows:

Extreme cold stress: UTCI below -40°C; Very strong cold stress: UTCI -40°C to -27°C; Strong

cold stress: UTCI -27°C to -13°C; Moderate cold stress: UTCI -13°C to 0°C; No thermal stress: UTCI 0°C to 26°C; Moderate heat stress: UTCI 26°C to 32°C; Strong heat stress: UTCI 32°C to 38°C; Very strong heat stress: UTCI 38°C to 46°C; Extreme heat stress: UTCI above 46°C;

B.2 Population data input specification

In each census year, we determine the population distribution by dividing the population of each age and gender group in each county by the entire population in the census year. For our analysis of children's exposure, we focus on the age group between 0 to 14 regardless of gender.

Census 1990 We obtained 2369 geographical units at the county level nested in 31 provincial administrative regions from the Tabulation on 1990 China Population Census by County. We start with the 1990 Chinese Census as it is the first to offer county-level population counts by ages 0-14. We only include mainland China and did not include special administrative regions. Within each county, we have population data by gender and age.

Census 2020 We obtained 2853 geographical units at the county level nested in 31 provincial administrative regions from the Tabulation on 2020 China Population Census by County. We only included mainland China and did not include special administrative regions. Within each county, we have population data by gender and age.

C Method Data Framework

C.1 ERA5-HEAT data input specification

We use the thermal comfort index, UTCI, derived from ERA5 reanalysis. This data, ERA5-HEAT, is publicly accessible through the Climate Data Store API service from the European Centre for Medium-Range Weather Forecasts. The ERA5-HEAT dataset provides hourly UTCI from January 1940 to near real-time in 0.25° by 0.25° (roughly 31 kilometers) latitude-longitude grid in NetCDF format.

To capture the entire mainland China area, we employ China's far-east (135°E), far-west (53°E), far-south (4°N), and far-north (54°N) points as spatial references in our API request to extract a rectangle area that contains gridded points with latitude and longitude coordinates

from the ERA5-HEAT data. For the time periods, We specify all months and dates in census years 1990, 2000, 2010, 2020 respectively in our API request. After having coordinate-specific hourly UTCI from all dates, we consolidate them into one data file by year. For example, in the 2020 data file, each coordinate in the gridded map includes hourly UTCI values from January 1, 2020 to December 31, 2020.

C.2 Population data input specification

We obtain county-level demographic data from the census tabulations. In each census file, there is one unique identification number for each county. Each county includes demographic data by age group and gender for the corresponding census year. The county shapefiles provide the geometry defining the boundaries of each county. This geometry is important for linking the population data with the gridded UTCI data.

The final population input consists of a data matrix. In this matrix, the first column signifies a distinct county ID, while other columns denote the proportion of the population by gender within specific 5-year age groups (ranging from 0-4 to 85+) relative to the total population of one census year. The heat exposure and share of children at risk are constructed considering only the age groups of 0-4, 5-9, and 10-14, combining data for both males and females. However, our approach has the flexibility to extend to any demographic group as needed.

C.3 Specifying key files

There are three key files necessary for linking population data input and UTCI input: (1) key file that links the coordinates to counties. (2) key file that links county to province and regions. (3) key file that links population input column variables to the original labels (e.g., age groups and gender), and grouping variables for aggregation purposes (i.e., age groups 0-14, 15-64, 65+).

Coordinates to counties. We use spatial join from the "sf" package in R to identify coordinates from UTCI data that fall within each county boundary.Some county units are too small to include any coordinates. In this case, we use the nearest coordinate to the centroid of the county geometry. The final key file includes a list of coordinates, with each coordinate labeled with the corresponding county code in China. The county code helps us link to the county-level population census, while the coordinates help us link to the ERA5-HEAT data.

County to province/region. Each county code can be linked back to the province and economic regions that the county belong to. In addition to province, we can easily aggregate the county to other higher level units.

Population input columns to labels. This key file provides label names to the population input columns.

D Additional Results on heat exposure for children

D.1 Average shares of time of heat exposure for children

In Tables D.1 and D.2, we present additional details on the change in average share of time at risk of exposure to heat stress thresholds for Chinese children (ages 0–14), between the years 1990 and 2020. We focus on the annual average share of time that Chinese children are exposed to UTCI temperature over thresholds $z\,^{\circ}$C. We group thresholds into four panels focusing at exposures to at least borderline thermal stress (23 °C–25 °C), to at least moderate heat stress (26 °C–31 °C), to at least strong heat stress (32 °C–37 °C), and to different thresholds of very strong heat exposure (38 °C–40 °C).

Table D.1's first four columns contain our main results where we consider ambient exposure during all hours of 1990 and 2020. The remaining four columns in Table D.1 present results considering only daytime (between 6 am and 10 pm) hours. Table D.2 presents results where we compare the average share of time at risk of exposure to heat stress thresholds in the warmer months of April, May, June, July, August and September with the colder months of January, February, March, October, November and December in 1990 and 2020.

What Tables D.1 and D.2 show is that the share of time at risk of exposure to heat stress thresholds for children is increasing across each threshold in which heat stress is present (i.e. Moderate, Strong, and Very Strong). Zooming further into Table D.1 and the result of 2.7 pp of increase in heat exposure $\geqslant 26\,^{\circ}$C, we note that this is not all due to increases in Moderate heat stress. This is evidenced by there being a 1.1 pp increase in heat exposure at $\geqslant 32\,^{\circ}$C. Jointly these results mean that approximately 60% $\left(\frac{2.7-1.1}{2.7} \approx 0.6\right)$ of the 2.7 pp comes from increases in Moderate heat exposure.

Further, in comparing the time differences in these results, there is approximately 30 to 50 percent higher share of time children are at risk of being exposed to heat stress in 2020 for daytime vs all day hours. This is a mechanical result, due to us dropping about 40 percent of the hours from the day $((24-14)/24)$. Additionally, there are between 14 and 18 percentage increases in shares of time at risk of exposure under Panels B and C for all hours, daytime only, as well as April-September results. October to March started in 1990 with very low levels of shares of time at risk of exposure to heat thresholds of average Very Strong and at Strong heat stress, and then experienced very large percentage increases.

Table D.1: Change in Average Share of Time at Risk of Exposure to Heat Stress Thresholds for Children, 1990 to 2020

	All annual hours $\geqslant$ UTCI thresholds				Day time (6 am-10 pm) hours $\geqslant$ UTCI thresholds			
	Share of time		Changes		Share of time		Changes	
UTCI thresholds	1990	2020	Level	%	1990	2020	Level	%
Panel a: Very strong heat stress								
$\geqslant$ 40 °C	0.3%	0.3%	0.0007pp	0.2%	0.4%	0.4%	0.001pp	0.2%
$\geqslant$ 39 °C	0.6%	0.6%	0.0pp	6.7%	0.9%	0.9%	0.1pp	6.7%
$\geqslant$ 38 °C	1.0%	1.2%	0.1pp	10.6%	1.6%	1.7%	0.2pp	10.7%
Panel b: At least strong heat stress								
$\geqslant$ 37 °C	1.7%	1.9%	0.3pp	15.1%	2.5%	2.9%	0.4pp	15.1%
$\geqslant$ 36 °C	2.5%	2.9%	0.4pp	17.3%	3.7%	4.4%	0.6pp	17.3%
$\geqslant$ 35 °C	3.4%	4.1%	0.6pp	18.1%	5.2%	6.1%	0.9pp	18.1%
$\geqslant$ 34 °C	4.6%	5.4%	0.8pp	17.5%	6.8%	8.0%	1.2pp	17.5%
$\geqslant$ 33 °C	5.8%	6.7%	0.9pp	16.1%	8.7%	10.1%	1.4pp	16.1%
$\geqslant$ 32 °C	7.2%	8.3%	1.1pp	14.7%	10.8%	12.3%	1.6pp	14.8%
Panel c: At least moderate heat stress								
$\geqslant$ 31 °C	8.7%	9.9%	1.2pp	13.9%	12.9%	14.7%	1.8pp	13.8%
$\geqslant$ 30 °C	10.4%	11.8%	1.4pp	13.6%	15.2%	17.3%	2.0pp	13.2%
$\geqslant$ 29 °C	12.3%	14.1%	1.7pp	14.0%	17.7%	20.0%	2.3pp	12.8%
$\geqslant$ 28 °C	14.6%	16.8%	2.2pp	14.8%	20.4%	22.9%	2.6pp	12.5%
$\geqslant$ 27 °C	17.2%	19.8%	2.5pp	14.8%	23.2%	26.0%	2.8pp	12.0%
$\geqslant$ 26 °C	20.1%	22.8%	2.7pp	13.5%	26.2%	29.1%	2.9pp	11.0%
Panel d: At least borderline thermal stress								
$\geqslant$ 25 °C	23.0%	25.7%	2.7pp	11.8%	29.3%	32.1%	2.8pp	9.7%
$\geqslant$ 24 °C	25.9%	28.6%	2.6pp	10.1%	32.3%	35.1%	2.7pp	8.5%
$\geqslant$ 23 °C	28.7%	31.3%	2.6pp	9.0%	35.3%	38.1%	2.7pp	7.7%

Note: Columns 1, 2, 5, and 6 show the annual average share of time at risk of exposure to heat stress thresholds (UTCI temperatures at $\geqslant z$ °C) for children in China (ages 0–14). Columns 3, 4, 7, and 8 show 1990 to 2020 changes in percentage points (level) or percentage (%) of the average shares of time exposed to heat. We consider both all hourly as well as only daytime hourly (between 6 am and 10 am) temperature data.

Table D.2: Change in Average Share of Time at Risk of Exposure to Heat Stress Thresholds for Children, during Warmer and Colder Months, 1990 to 2020

	April–September hours ⩾ UTCI thresholds				October–March hours ⩾ UTCI thresholds			
	Share of time		Changes		Share of time		Changes	
UTCI thresholds	1990	2020	Level	%	1990	2020	Level	%
Panel a: Very strong heat stress								
⩾ 40 °C	0.6%	0.6%	0.001pp	0.2%	0.00002%	0.00008%	0.00006pp	334.3%
⩾ 39 °C	1.2%	1.2%	0.1pp	6.6%	0.0001%	0.0004%	0.0002pp	159.0%
⩾ 38 °C	2.1%	2.3%	0.2pp	10.6%	0.0004%	0.002%	0.001pp	373.7%
Panel b: At least strong heat stress								
⩾ 37 °C	3.3%	3.8%	0.5pp	14.9%	0.002%	0.010%	0.008pp	476.0%
⩾ 36 °C	4.9%	5.8%	0.8pp	17.0%	0.006%	0.02%	0.0pp	291.4%
⩾ 35 °C	6.9%	8.1%	1.2pp	17.7%	0.02%	0.05%	0.0pp	144.1%
⩾ 34 °C	9.0%	10.6%	1.6pp	17.1%	0.06%	0.10%	0.0pp	67.0%
⩾ 33 °C	11.5%	13.3%	1.8pp	15.8%	0.1%	0.2%	0.0pp	35.1%
⩾ 32 °C	14.1%	16.2%	2.1pp	14.7%	0.3%	0.3%	0.0pp	14.1%
Panel c: At least moderate heat stress								
⩾ 31 °C	16.9%	19.3%	2.4pp	14.2%	0.5%	0.5%	0.0pp	4.2%
⩾ 30 °C	20.0%	22.8%	2.8pp	14.1%	0.8%	0.8%	0.0pp	2.5%
⩾ 29 °C	23.4%	26.9%	3.4pp	14.6%	1.2%	1.2%	0.0pp	3.0%
⩾ 28 °C	27.5%	31.7%	4.3pp	15.5%	1.7%	1.7%	0.1pp	3.4%
⩾ 27 °C	32.0%	37.0%	5.0pp	15.6%	2.4%	2.4%	0.1pp	2.8%
⩾ 26 °C	36.9%	42.2%	5.3pp	14.5%	3.2%	3.3%	0.1pp	2.5%
Panel d: At least borderline thermal stress								
⩾ 25 °C	41.7%	47.0%	5.3pp	12.7%	4.2%	4.4%	0.1pp	2.7%
⩾ 24 °C	46.3%	51.4%	5.1pp	11.0%	5.4%	5.6%	0.2pp	3.0%
⩾ 23 °C	50.6%	55.5%	4.9pp	9.7%	6.8%	7.1%	0.3pp	4.0%

Note: Columns 1, 2, 5, and 6 show the annual average share of time at risk of exposure to heat stress thresholds (UTCI temperatures at ⩾ z °C) for children in China (ages 0–14). Columns 3, 4, 7, and 8 show 1990 to 2020 changes in percentage points (level) or percentage (%) of the average shares of time exposed to heat. We compare temperatures across time for April, May, June, July, August and September and then for January, February, March, October, November and December of each year. We consider all 24 hours.

D.2 Share of children at risk of heat exposure

In Tables D.3 and D.4, we present additional details from the analysis of the minimal share of children at risk of exposure to heat stress thresholds, considering the double thresholds of intensity (UTCI temperature thresholds $z\,^{\circ}$C) and duration (share of time in year thresholds $y\%$). In each scenario, the share of children is computed by aggregating the share of the child population from locations (counties) experiencing these double thresholds of exposure.

In both Tables D.3 and D.4, across the columns, we present 9 duration thresholds, starting with at least 2 weeks or half a month of heat exposure (approximately 4% of a year's time) and ending with at least 18 weeks or 4.1 months (approximately 36% of a year's time) of exposure. Across the rows, we consider UTCI thresholds including a number of at least Moderate and at least Strong heat stress thresholds. In Table D.3, Panels A and B present shares of children at risk in 1990 and 2020. In Table D.3, Panels A and B present percentage points and percentage changes between 1990 and 2020.

In Table D.3, we show that at least some children in China during the year 1990 experienced at least some amount of Moderate heat stress ($\geqslant 26\,^{\circ}$C) for as little as two weeks to as long as eighteen weeks: 97.2% of children and 6.7% of children respectively. By 2020, the percentage of children experiencing at least Moderate heat stress increased across all weekly intervals: 97.7% and 13.7% of children respectively. The change in children experiencing at least Moderate heat stress for eighteen weeks or 36% of their year has more than doubled, as depicted in Table D.4 Panel B. Looking only two degrees higher while still within the category of Moderate heat stress ($\geqslant 28\,^{\circ}$C), this change is even more dramatic: 3.8% of children in 2020 experienced $\geqslant 28\,^{\circ}$C for three months, 38 times higher than 0.1% (several hundred thousand) children in 1990.

Looking at the higher heat stress thresholds in both Table D.3 and Table D.4 Panel B, like Strong heat stress ($\geqslant 32\,^{\circ}$C) we also show broad increases in the percentage of children exposed, although for not as many weekly time intervals in either 1990 or 2020. We estimate that for at least two weeks, 72.7% of children in China experienced at least Strong heat stress ($\geqslant 32\,^{\circ}$C) in 1990. By 2020, this minimal Strong heat stress threshold was met by 77.8% of children. While no child in either 1990 nor 2020 experienced more than ten weeks of Strong heat stress ($\geqslant 32\,^{\circ}$C), those ten weeks of Strong heat stress or more than 20% of a year were felt by 0.1% of children in 1990 and six times as many children in 2020.

Between 1990 and 2020, the percentage of children experiencing multiple heat stress thresholds increased across new time interval thresholds. For the higher thresholds of at least Moderate heat stress($\geqslant 30\,^{\circ}$C), the maximum time interval where any child experienced heat stress was twelve weeks ($\geqslant$ 24% of the year), by 2020 some amount of children were experiencing sixteen weeks ($\geqslant$ 32% of the year) under at least Moderate heat stress ($\geqslant 30\,^{\circ}$C). In the middle and higher ends of at least Strong heat stress ($\geqslant 34\,^{\circ}$C and $\geqslant 36\,^{\circ}$C), the maximum amount of time children experienced these levels of heat stress rose from eight to ten weeks, and four to six weeks ($\geqslant$ 8% to $\geqslant$ 12% of the year) respectively. Finally, at Very Strong heat stress ($\geqslant 38\,^{\circ}$C), the same percentage of children that experienced the maximum time interval of two weeks ($\geqslant$ 4% of the year) in 1990, then reached a new maximum time interval in 2020 of four weeks of exposure ($\geqslant$ 8% of the year).

Table D.3: Share of Children at Risk of Exposure to Heat Stress Thresholds, 1990 to 2020

	Minimal share of time in year thresholds and corresponding number of weeks								
	$\geqslant$ 4%	$\geqslant$ 8%	$\geqslant$ 12%	$\geqslant$ 16%	$\geqslant$ 20%	$\geqslant$ 24%	$\geqslant$ 28%	$\geqslant$ 32%	$\geqslant$ 36%
UTCI thresholds	2 weeks	4 weeks	6 weeks	8 weeks	10 wks	12 wks	14 wks	16 wks	18 wks
Panel a: 1990									
x% (cell) of children with at least y% (column) of time in year 1990 at $\geqslant z$ °C (row) heat threshold									
Very strong heat stress									
$\geqslant$ 38 °C	0.1%								
At least strong heat stress									
$\geqslant$ 36 °C	27.2%	0.1%							
$\geqslant$ 34 °C	60.1%	15.1%	0.5%						
$\geqslant$ 32 °C	72.7%	52.1%	11.2%	1.4%	0.1%				
At least moderate heat stress									
$\geqslant$ 30 °C	80.9%	69.0%	43.7%	13.1%	4.5%	0.4%			
$\geqslant$ 28 °C	91.4%	77.5%	68.0%	44.6%	19.5%	7.5%	4.5%	1.4%	0.1%
$\geqslant$ 26 °C	97.2%	87.0%	76.6%	68.5%	54.4%	31.1%	16.3%	8.6%	6.7%
At least borderline thermal stress									
$\geqslant$ 24 °C	98.8%	96.0%	84.9%	76.6%	70.8%	63.2%	44.2%	25.3%	13.9%
Panel b: 2020									
x% (cell) of children with at least y% (column) of time in year 2020 at $\geqslant z$ °C (row) heat threshold									
Very strong heat stress									
$\geqslant$ 38 °C	1.8%	0.1%							
At least strong heat stress									
$\geqslant$ 36 °C	32.4%	2.1%	0.2%						
$\geqslant$ 34 °C	66.6%	20.1%	3.4%	0.4%					
$\geqslant$ 32 °C	77.8%	59.1%	18.6%	6.1%	0.6%				
At least moderate heat stress									
$\geqslant$ 30 °C	86.0%	75.6%	52.9%	20.7%	10.4%	3.0%	0.5%	0.1%	
$\geqslant$ 28 °C	94.3%	83.5%	74.6%	53.6%	25.9%	17.4%	10.9%	7.4%	3.8%
$\geqslant$ 26 °C	97.7%	91.9%	81.4%	74.5%	59.7%	34.8%	24.9%	17.9%	13.7%
At least borderline thermal stress									
$\geqslant$ 24 °C	98.7%	97.0%	89.7%	81.2%	76.4%	65.6%	45.1%	32.4%	23.3%

Note: Cells show the shares of Chinese children (ages 0–14) experiencing at least y% of their time in a year at risk of exposure to at least a particular z °C UTCI temperature threshold. Shares of children at risk are computed based on aggregating population shares from locations (counties) experiencing the various combinations of heat stress duration (share of time) and intensity (temperature) thresholds. For minimal shares of time in a year, the correspondence between the share of time and the number of weeks is based on the fact that the average of N weeks of time and $\frac{N}{4}$ months of time is approximately $(N \cdot 2)$% of total share of time in a year. To enhance contrast, values are rounded and cells with values less than 0.05% or 0.05pp are left empty. We consider all 24 hours and 12 months.

Table D.4: Change in Share of Children at Risk of Exposure to Heat Stress Thresholds, 2020-1990

	Minimal share of time in year thresholds and corresponding number of weeks								
	$\geqslant 4\%$	$\geqslant 8\%$	$\geqslant 12\%$	$\geqslant 16\%$	$\geqslant 20\%$	$\geqslant 24\%$	$\geqslant 28\%$	$\geqslant 32\%$	$\geqslant 36\%$
UTCI thresholds	2 weeks	4 weeks	6 weeks	8 weeks	10 wks	12 wks	14 wks	16 wks	18 wks
Panel a: 2020% − 1990%									
Increases in percentage points (cell) of children with at least y% (column) of time at $\geqslant z$ °C (row) heat threshold									
Very strong heat stress									
$\geqslant 38$ °C	1.7pp	0.1pp							
At least strong heat stress									
$\geqslant 36$ °C	5.2pp	2.0pp	0.2pp						
$\geqslant 34$ °C	6.6pp	5.0pp	2.9pp	0.4pp					
$\geqslant 32$ °C	5.1pp	6.9pp	7.4pp	4.7pp	0.5pp				
At least moderate heat stress									
$\geqslant 30$ °C	5.2pp	6.5pp	9.2pp	7.6pp	6.0pp	2.6pp	0.5pp	0.1pp	
$\geqslant 28$ °C	2.8pp	6.0pp	6.6pp	8.9pp	6.4pp	9.9pp	6.4pp	6.0pp	3.8pp
$\geqslant 26$ °C	0.6pp	5.0pp	4.8pp	6.0pp	5.2pp	3.7pp	8.6pp	9.3pp	7.0pp
At least borderline thermal stress									
$\geqslant 24$ °C	-0.2pp	1.0pp	4.8pp	4.6pp	5.5pp	2.5pp	0.9pp	7.2pp	9.4pp
Panel b: $\frac{2020\%-1990\%}{1990\%} \cdot 100$									
Percentage increases (cell) of children with at least y% (column) of time at $\geqslant z$ °C (row) heat threshold									
Very strong heat stress									
$\geqslant 38$ °C	1.8k%								
At least strong heat stress									
$\geqslant 36$ °C	19.2%	2.3k%							
$\geqslant 34$ °C	10.9%	33.1%	606%						
$\geqslant 32$ °C	7.0%	13.3%	66.3%	330%	792%				
At least moderate heat stress									
$\geqslant 30$ °C	6.4%	9.4%	20.9%	58.5%	133%	654%			
$\geqslant 28$ °C	3.1%	7.7%	9.7%	20.0%	32.9%	131%	141%	414%	5.2k%
$\geqslant 26$ °C	0.6%	5.7%	6.3%	8.7%	9.6%	11.7%	52.9%	109%	106%
At least borderline thermal stress									
$\geqslant 24$ °C	-0.2%	1.0%	5.7%	6.0%	7.8%	3.9%	2.1%	28.5%	67.5%

Note: Cells show changes between 1990 and 2020 in percentage points (Panel A) and percentage (Panel B) of the shares of Chinese children (ages 0–14) experiencing at least y% of their time in a year at risk of exposure to at least a particular z °C UTCI temperature threshold. Shares of children at risk are computed based on aggregating population shares from locations (counties) experiencing the various combinations of heat stress duration (share of time) and intensity (temperature) thresholds. For minimal shares of time in a year, the correspondence between the share of time and the number of weeks is based on the fact that the average of N weeks of time and $\frac{N}{4}$ months of time is approximately $(N \cdot 2)$% of total share of time in a year. To enhance contrast, values are rounded and cells with values less than 0.05% or 0.05pp are left empty. We consider all 24 hours and 12 months.

D.3 Decomposition shifting only population or temperature distributions

In this section, we provide more details on the relative contributions of shifts in the child population distribution and the temperature distribution to overall changes in average share time exposed to heat. Our decomposition analysis is statistical in nature: we shift one distribution while holding the other constant and do not model mechanisms of change. Also note that actual changes unexplained by the sum of population and temperature decompositions are attributable to population and temperature interactions.

Following Table D.1, columns 1–3 of Table D.5 include actual annual average shares of time that children risk exposure to UTCI temperatures at $\geqslant z$ °C and percentage points changes over time. In columns 4–6, we compute exposures using the 1990 population distribution jointly with the 2020 UTCI temperature distribution. In columns 7–9, we consider exposures if the 2020 population distribution faced the 1990 UTCI temperature distribution. We present in Panel A national results. Panels B and C show results in the Eastern and Northeastern regions which experienced large increases in heat exposure (see Table D.7).

In Table D.5 we show the importance of noting population shifts alongside temperature effects. For at least Strong ($\geqslant$ 32 °C) heat stress levels, child population distribution shifts nationally account for 48% (and 29% in the Eastern and 9% in the Northeastern region) and 50% (38%/16%) of at least Moderate heat stress ($\geqslant$ 26 °C) change, respectively. In contrast, temperature distribution shifts account for 42% (61%/92%) and 40% (51%/81%) of the heat exposure changes, respectively. For Central and Western regions of China in Panels A and B Table D.6, population effects are less consistently greater than temperature effects, only being greater in Western China at Strong ($\geqslant$ 32 °C) heat stress levels (68% versus 54%), and at higher Strong heat stress thresholds ($\geqslant$ 36 °C) (27% versus -33%)

Second, we observe the importance of cross-regional movement in Tables D.5 and D.6 for at least Moderate heat stress ($\geqslant$ 26 °C)on the National, Eastern , Northeastern, Central, and Western regions , where population shifts account for 50%, 38%, 16%, 21%, and -326% of the actual exposure shifts in their respective geographies. The national results are due to shifts within and across regions, whereas the regional results are attributed to only within-region shifts.

Finally, in the last column of Tables D.5 and D.6 we note the decreased importance of population effects at higher UTCI thresholds. Contribution of population distribution generally

decreases with increasing heat stress thresholds: nationally (in Eastern/Northeastern/Western regions) from 61% (53%/20%/2,174,605%) at borderline heat stress of $\geqslant$ 24 °C to 39% (19%/5%/49%) at higher levels of Strong heat stress $\geqslant$ 36 °C. Increases in the higher heat exposures come more from increasing temperatures rather than from populations moving to locations that were already hotter in 1990.

Table D.5: Decomposed Change in Average Share of Time Children Exposed to Heat

	Actual 2020 vs 1990			2020 UTCI with 1990 population			1990 UTCI with 2020 population		
	Share of time		Changes	Share-time	Decompose changes		Share-time	Decompose changes	
UTCI thresholds	1990	2020	Δ	Prediction	Vs. 1990	% of Δ	Prediction	Vs. 1990	% of Δ
Panel a: National									
At least strong heat stress									
$\geqslant 36\,^{\circ}C$	2.5%	2.9%	0.43pp	2.7%	0.17pp	40%	2.7%	0.17pp	39%
$\geqslant 34\,^{\circ}C$	4.6%	5.4%	0.80pp	4.9%	0.35pp	45%	4.9%	0.33pp	42%
$\geqslant 32\,^{\circ}C$	7.2%	8.3%	1.06pp	7.6%	0.44pp	42%	7.7%	0.51pp	48%
At least moderate heat stress									
$\geqslant 30\,^{\circ}C$	10.4%	11.8%	1.42pp	11.0%	0.60pp	42%	11.1%	0.69pp	49%
$\geqslant 28\,^{\circ}C$	14.6%	16.8%	2.16pp	15.5%	0.90pp	42%	15.6%	0.98pp	45%
$\geqslant 26\,^{\circ}C$	20.1%	22.8%	2.72pp	21.2%	1.08pp	40%	21.4%	1.35pp	50%
At least borderline thermal stress									
$\geqslant 24\,^{\circ}C$	25.9%	28.6%	2.63pp	26.8%	0.88pp	33%	27.5%	1.60pp	61%
Panel b: Eastern region									
At least strong heat stress									
$\geqslant 36\,^{\circ}C$	2.7%	3.5%	0.85pp	3.3%	0.59pp	70%	2.9%	0.16pp	19%
$\geqslant 34\,^{\circ}C$	5.3%	6.6%	1.35pp	6.1%	0.89pp	66%	5.6%	0.31pp	23%
$\geqslant 32\,^{\circ}C$	8.4%	10.1%	1.70pp	9.5%	1.03pp	61%	8.9%	0.50pp	29%
At least moderate heat stress									
$\geqslant 30\,^{\circ}C$	12.1%	14.3%	2.26pp	13.4%	1.33pp	59%	12.8%	0.73pp	32%
$\geqslant 28\,^{\circ}C$	17.0%	20.7%	3.70pp	19.0%	2.02pp	55%	18.2%	1.18pp	32%
$\geqslant 26\,^{\circ}C$	23.6%	28.1%	4.44pp	25.9%	2.27pp	51%	25.3%	1.69pp	38%
At least borderline thermal stress									
$\geqslant 24\,^{\circ}C$	30.6%	34.2%	3.54pp	32.0%	1.36pp	38%	32.5%	1.87pp	53%
Panel c: Northeastern region									
At least strong heat stress									
$\geqslant 36\,^{\circ}C$	0.04%	0.3%	0.27pp	0.3%	0.24pp	89%	0.05%	0.01pp	5%
$\geqslant 34\,^{\circ}C$	0.3%	1.1%	0.79pp	1.%	0.72pp	91%	0.3%	0.05pp	6%
$\geqslant 32\,^{\circ}C$	1.1%	2.4%	1.22pp	2.3%	1.12pp	92%	1.3%	0.11pp	9%
At least moderate heat stress									
$\geqslant 30\,^{\circ}C$	2.8%	4.1%	1.35pp	4.0%	1.23pp	91%	2.9%	0.17pp	13%
$\geqslant 28\,^{\circ}C$	5.0%	6.4%	1.39pp	6.2%	1.21pp	87%	5.2%	0.21pp	15%
$\geqslant 26\,^{\circ}C$	7.5%	8.9%	1.43pp	8.7%	1.16pp	81%	7.7%	0.24pp	16%
At least borderline thermal stress									
$\geqslant 24\,^{\circ}C$	10.4%	11.8%	1.45pp	11.4%	1.06pp	73%	10.7%	0.29pp	20%

Note: Columns (cols) 1–3 include actual annual average share of time that children in China (ages 0–14) are at risk of exposure to UTCI temperatures at $\geqslant z\,^{\circ}C$ (same information as cols 1–3 in Table D.1). Cols 4–6 consider heat exposure if the 1990 population distribution faced the 2020 UTCI temperature distribution. Cols 7–9 consider exposure if 2020 population faced 1990 UTCI temperatures. Cols 4 and 7 show predictions of annual average shares of time exposed to heat thresholds given decomposition scenarios. Cols 5 and 8 show differences between predictions and 1990 actual average shares. Cols 6 and 9 show the share of column 3 actual changes that the predictions from cols 5 and 8 account for. See Table D.7 for provincial-level administrative units in the Eastern and Northeastern regions. We consider all 24 hours and 12 months.

Table D.6: Decomposed Change in Average Share of Time Children Exposed to Heat

	Actual 2020 vs 1990			2020 UTCI with 1990 population			1990 UTCI with 2020 population		
	Share of time		Changes	Share-time	Decompose changes		Share-time	Decompose changes	
UTCI thresholds	1990	2020	Δ	Prediction	Vs. 1990	% of Δ	Prediction	Vs. 1990	% of Δ
Panel A: Central region									
At least strong heat stress									
$\geqslant 36\,^{\circ}$C	3.7%	3.7%	0.08pp	3.6%	-0.03pp	-33%	3.7%	0.02pp	27%
$\geqslant 34\,^{\circ}$C	6.2%	6.5%	0.25pp	6.4%	0.11pp	45%	6.3%	0.03pp	14%
$\geqslant 32\,^{\circ}$C	9.3%	9.6%	0.30pp	9.4%	0.13pp	43%	9.3%	0.04pp	14%
At least moderate heat stress									
$\geqslant 30\,^{\circ}$C	12.9%	13.3%	0.39pp	13.1%	0.21pp	53%	12.9%	0.04pp	10%
$\geqslant 28\,^{\circ}$C	17.6%	17.9%	0.38pp	17.8%	0.19pp	51%	17.6%	0.03pp	9%
$\geqslant 26\,^{\circ}$C	23.4%	23.6%	0.21pp	23.4%	0.04pp	22%	23.4%	0.04pp	21%
At least borderline thermal stress									
$\geqslant 24\,^{\circ}$C	29.2%	29.6%	0.42pp	29.5%	0.27pp	64%	29.3%	0.08pp	19%
Panel B: Western region									
At least strong heat stress									
$\geqslant 36\,^{\circ}$C	1.8%	1.7%	-0.17pp	1.7%	-0.15pp	84%	1.7%	-0.08pp	49%
$\geqslant 34\,^{\circ}$C	3.5%	3.3%	-0.21pp	3.3%	-0.14pp	68%	3.4%	-0.14pp	65%
$\geqslant 32\,^{\circ}$C	5.7%	5.4%	-0.30pp	5.6%	-0.16pp	54%	5.5%	-0.20pp	68%
At least moderate heat stress									
$\geqslant 30\,^{\circ}$C	8.5%	8.2%	-0.31pp	8.5%	-0.08pp	25%	8.2%	-0.31pp	99%
$\geqslant 28\,^{\circ}$C	12.2%	12.1%	-0.14pp	12.4%	0.20pp	-141%	11.8%	-0.42pp	302%
$\geqslant 26\,^{\circ}$C	17.1%	17.2%	0.18pp	17.8%	0.71pp	400%	16.5%	-0.58pp	-326%
At least borderline thermal stress									
$\geqslant 24\,^{\circ}$C	22.7%	22.7%	-	23.5%	0.87pp	-	21.8%	-0.83pp	2,174,605%
			0.00004pp			2,280,906%			

Note: Columns (cols) 1–3 include actual annual average share of time that children in China (ages 0–14) are at risk of exposure to UTCI temperatures at $\geqslant z\,^{\circ}$C (same information as cols 1–3 in Table D.1). Cols 4–6 consider heat exposure if the 1990 population distribution faced the 2020 UTCI temperature distribution. Cols 7–9 consider exposure if 2020 population faced 1990 UTCI temperatures. Cols 4 and 7 show predictions of annual average shares of time exposed to heat thresholds given decomposition scenarios. Cols 5 and 8 show differences between predictions and 1990 actual average shares. Cols 6 and 9 show the share of column 3 actual changes that the predictions from cols 5 and 8 account for. See Table D.7 for provincial-level administrative units in the Eastern and Northeastern regions. We consider all 24 hours and 12 months.

D.4 Additional regional analysis

In this section, we augment the region-specific heat exposure analysis with province-specific analysis as well. Similar to Table D.7, we analyze changes in the average share of time at risk of heat exposure between 1990 and 2020 for Chinese children (ages 0-14). Overall national, regional, and provincial changes are due to shifts over time in both the temperature distribution and the child population distribution across space within the country, region, or province. Sub-national analyses not only show which areas are experiencing greater changes in heat exposures but also shed light on whether aggregate national and regional changes are due to population shifts across regions and across provinces within-region, respectively. [D.1]

In Panel A of Tables D.7 and D.8, we conduct our analysis based on changes in the distribution of children and temperature within each of the four economic regions of China. In successive panels, we present province-specific results based on within-province changes. Table D.7 presents results for at least Strong ($\geqslant 32\,^{\circ}$C and $\geqslant 35\,^{\circ}$C) and Very Strong heat stress ($\geqslant 38\,^{\circ}$C) exposure thresholds across columns. Table D.8 focuses on Moderate ($\geqslant 26\,^{\circ}$C and $\geqslant 29\,^{\circ}$C) heat stress thresholds and also provides results for the $\geqslant 23^{\circ}$C threshold.

In Panel A of Tables D.7 and D.8 we show that in 1990, the Central region, followed by the Eastern, had the highest average share of child heat exposure time. Between 1990 and 2020, while Central exposure stagnated with 1% to 4% increases (for at least Moderate and Strong heat stress thresholds), the Eastern region experienced increases of 20% to 35% across heat stress thresholds, catching up to the central region. In 2020, the average Eastern region child experienced 28.1% and 10.1% of her time under at least Moderate ($\geqslant 26\,^{\circ}$C) and at least Strong ($\geqslant 32\,^{\circ}$C) heat stress. Meanwhile, the Northeastern region had very low average child heat exposure in 1990, but by 2020, experienced increases of 19% ($\geqslant 26\,^{\circ}$C) and 36% ($\geqslant 29\,^{\circ}$C) for average at least Moderate heat stress and 106% ($\geqslant 32\,^{\circ}$C) and 457% ($\geqslant 35\,^{\circ}$C) for at least Strong heat stress. In 2020, the average Northeastern region child experienced 8.9% and 2.4% of her time under at least Moderate ($\geqslant 26\,^{\circ}$C) and at least strong ($\geqslant 32\,^{\circ}$C) heat stress, which are still much lower than average exposure levels in Central and Eastern regions.

In Panels B-D of Tables D.7 and D.8 we observe different levels of temperature exposure for children across provinces within the regions of China. In 2020, Hainan (Eastern), Guangdong (Eastern), Guangxi (Western), Jiangxi (Central), and Fujian (Eastern) are generally ranked from

D.1. In an extreme scenario, there might be no changes in temperatures and no changes in the distribution of population within regions, but if the overall national population shares in higher heat stress regions increase, average national child heat exposure will increase.

top 1 to 5 in terms of average share of child time exposed to heat across all UTCI thresholds. Specifically, in 2020, children in Hainan, Guangdong, Guangxi, Jiangxi and Fujian had on average 19.2%, 15.2%, 13.2%, 12.8%, and 11.8% share of time exposed to at least Strong heat stress ($\geqslant 32\,^{\circ}$C), which represented respective increases of 17%, 20%, 8%, 16%, and 54% in share of time exposed compared to 1990.

On the opposite end of Panels B-D of Tables D.7 and D.8, we also observe some cases of decreasing heat exposure. While Northeastern and Eastern provinces (excluding Jiangsu) experienced substantial increases in heat exposure, provinces in Central and Western regions experienced limited exposure increases and reductions. In particular, Central China's provinces of Hubei and Anhui and Western China's provinces of Shaanxi and Sichuan generally experienced reductions in average child heat exposures across UTCI thresholds. Additionally, children in Qinghai and Xizang (Tibet) in the Western region continue to have generally no exposure to at least Moderate heat stress.

Lastly, we note the extent to which provinces have similar changes in exposure. For at least Strong heat stress ($\geqslant 32\,^{\circ}$C), Hebei and Zhejiang in the Eastern region, along with all Northeastern provinces, all experienced between 1.0 to 1.3 percentage points increases in average share of time heat exposure. Since the Northeastern provinces started at much lower levels, the percentage increases in the Northeastern provinces are 3 to 15 times larger. Due to heterogeneities across provinces in prior exposure levels, the same percentage points increases represented a much bigger change from the status quo for the Northeastern provinces. Other nuance is also notable in comparing provinces. In 2020, the average child experienced 7.6% and 7.8% of her annual time with at least Strong heat stress ($\geqslant 32\,^{\circ}$C) in the Eastern provinces of Hebei and Jiangsu, respectively. But Hebei and Jiangsu experienced a 17% increase and an 11% reduction in heat exposure between 1990 and 2020, respectively. Depending on prior exposure levels, provinces might require different types of societal and physical adjustments despite having the same level of heat exposure today.

D.4.1 Very Strong and Strong heat stress across regions

Table D.7: Regional Average Share of Time at Risk of Exposure to Strong and Very Strong Heat Stress Thresholds for Children (ages 0-14), 1990 to 2020

	At least strong heat stress								Very strong heat stress			
	⩾ UTCI 32° C				⩾ UTCI 35° C				⩾ UTCI 38° C			
	Share of time		Changes		Share of time		Changes		Share of time		Changes	
Location	1990	2020	Level	%	1990	2020	Level	%	1990	2020	Level	%
Panel a: Regions												
Eastern	8.4%	10.1%	1.7pp	20%	3.9%	5.0%	1.1pp	29%	1.0%	1.4%	0.4pp	35%
Northeastern	1.1%	2.4%	1.2pp	106%	0.1%	0.6%	0.5pp	457%	0.0%	0.1%	0.1pp	7.4k%
Central	9.3%	9.6%	0.3pp	3%	4.9%	5.1%	0.2pp	4%	1.7%	1.6%	-0.1pp	-3%
Western	5.7%	5.4%	-0.3pp	-5%	2.6%	2.4%	-0.2pp	-7%	0.8%	0.6%	-0.2pp	-24%
Panel b: Eastern region												
Beijing	2.9%	6.3%	3.4pp	117%	0.5%	2.8%	2.3pp	424%	0.0%	0.6%	0.6pp	1.2k%
Fujian	7.7%	11.8%	4.1pp	54%	2.9%	5.6%	2.7pp	94%	0.5%	1.3%	0.9pp	175%
Guangdong	12.7%	15.2%	2.5pp	20%	5.7%	7.5%	1.8pp	31%	1.3%	2.0%	0.7pp	56%
Hainan	16.3%	19.2%	2.8pp	17%	6.4%	10.0%	3.6pp	57%	0.9%	3.4%	2.4pp	261%
Hebei	6.5%	7.6%	1.1pp	17%	2.9%	3.9%	1.0pp	34%	0.8%	1.0%	0.2pp	31%
Jiangsu	8.7%	7.8%	-0.9pp	-11%	4.7%	3.8%	-0.9pp	-20%	1.7%	1.3%	-0.4pp	-25%
Shandong	6.8%	7.1%	0.4pp	6%	2.9%	3.3%	0.4pp	13%	0.5%	0.9%	0.3pp	58%
Shanghai	6.8%	6.1%	-0.7pp	-10%	3.1%	2.7%	-0.4pp	-14%	1.0%	0.6%	-0.4pp	-40%
Tianjin	5.6%	7.3%	1.7pp	31%	2.1%	3.8%	1.7pp	84%	0.2%	0.9%	0.7pp	308%
Zhejiang	8.2%	9.2%	1.0pp	12%	4.6%	4.9%	0.4pp	8%	1.9%	1.6%	-0.3pp	-14%
Panel c: Northeastern region												
Heilongjiang	0.6%	1.7%	1.1pp	175%	0.0%	0.4%	0.4pp	1.6k%	0.0%	0.0%	0.0pp	
Jilin	0.8%	2.1%	1.3pp	148%	0.0%	0.5%	0.5pp	2.7k%	0.0%	0.0%	0.0pp	
Liaoning	1.9%	2.9%	1.1pp	56%	0.3%	0.8%	0.6pp	216%	0.0%	0.1%	0.1pp	4.5k%
Panel d: Central region												
Anhui	10.1%	9.3%	-0.8pp	-7%	5.8%	5.0%	-0.9pp	-15%	2.2%	1.8%	-0.4pp	-18%
Henan	8.9%	9.5%	0.6pp	7%	4.5%	5.1%	0.5pp	12%	1.4%	1.6%	0.2pp	13%
Hubei	10.2%	9.3%	-0.9pp	-9%	5.5%	4.9%	-0.6pp	-10%	2.0%	1.3%	-0.7pp	-35%
Hunan	10.2%	10.6%	0.4pp	4%	5.0%	5.4%	0.4pp	7%	1.6%	1.6%	0.0pp	0%
Jiangxi	11.0%	12.8%	1.8pp	16%	6.1%	7.4%	1.2pp	20%	2.4%	2.9%	0.5pp	19%
Shanxi	2.6%	2.8%	0.1pp	5%	0.8%	0.7%	-0.1pp	-18%	0.2%	0.1%	-0.1pp	-53%
Panel e: Western region												
Gansu	0.8%	0.8%	0.0pp	-1%	0.1%	0.1%	0.0pp	-17%	0.0%	0.0%	0.0pp	-17%
Guangxi	12.3%	13.2%	1.0pp	8%	5.5%	6.6%	1.1pp	20%	1.5%	1.4%	-0.1pp	-7%
Guizhou	2.8%	2.1%	-0.7pp	-26%	0.7%	0.3%	-0.4pp	-53%	0.1%	0.0%	0.0pp	-54%
Neimenggu	0.9%	2.0%	1.1pp	116%	0.1%	0.6%	0.4pp	296%	0.0%	0.1%	0.1pp	268%

Continued on next page

Table D.7: Regional Average Share of Time at Risk of Exposure to Strong and Very Strong Heat Stress Thresholds for Children (ages 0-14), 1990 to 2020

	At least strong heat stress								Very strong heat stress			
	⩾ UTCI 32° C				⩾ UTCI 35° C				⩾ UTCI 38° C			
	Share of time		Changes		Share of time		Changes		Share of time		Changes	
Location	1990	2020	Level	%	1990	2020	Level	%	1990	2020	Level	%
Ningxia	2.1%	2.8%	0.7pp	31%	0.7%	0.9%	0.2pp	35%	0.1%	0.1%	0.0pp	17%
Qinghai	0.0%	0.0%	0.0pp		0.0%	0.0%	0.0pp		0.0%	0.0%	0.0pp	
Shaanxi	4.6%	4.3%	-0.4pp	-8%	1.9%	1.5%	-0.4pp	-23%	0.6%	0.2%	-0.3pp	-58%
Sichuan	8.0%	7.4%	-0.7pp	-8%	4.2%	3.6%	-0.6pp	-14%	1.3%	1.0%	-0.3pp	-23%
Xinjiang	4.3%	5.2%	0.9pp	22%	2.0%	2.4%	0.4pp	19%	0.7%	0.7%	0.0pp	0%
Xizang	0.0%	0.0%	0.0pp		0.0%	0.0%	0.0pp		0.0%	0.0%	0.0pp	
Yunnan	0.9%	1.2%	0.3pp	33%	0.1%	0.1%	0.0pp	53%	0.0%	0.0%	0.0pp	-7%

Note: We present similar statistics as in Table D.1, but now compute exposures separately for four economic regions and provincial-level administrative units in China. Columns (cols) 1–3 and 4–6 focus on at least Strong UTCI heat exposure at ⩾ 32 °C and ⩾ 35 °C, respectively. Cols 7–9 focus on Very Strong UTCI heat exposure at ⩾ 38 °C. Cols 1 and 2, 5 and 6, and 9 and 10 show the annual average share of time at risk of exposure to heat stress thresholds (UTCI temperatures at ⩾ z °C) for children in China (ages 0–14). Cols 3 and 4, 7 and 8, and 11 and 12 show 1990 to 2020 changes in percentage points (level) or percentage (%) of the average shares of time exposed to heat. Cells are empty for percentage changes when the denominator is equal to zero. We consider all 24 hours and 12 months.

D.4.2 Moderate and No Heat Stress across regions

Table D.8: Regional Average Share of Time at Risk of Exposure to Moderate Heat Stress Thresholds for Children (ages 0-14), 1990 to 2020

	At least borderline thermal stress				At least moderate heat stress							
	⩾ UTCI 23° C				⩾ UTCI 26° C				⩾ UTCI 29° C			
	Share of time		Changes		Share of time		Changes		Share of time		Changes	
Location	1990	2020	Level	%	1990	2020	Level	%	1990	2020	Level	%
Panel a: Regions												
Eastern	33.8%	37.0%	3.2pp	9%	23.6%	28.1%	4.4pp	19%	14.3%	17.1%	2.8pp	20%
Northeastern	12.0%	13.5%	1.5pp	13%	7.5%	8.9%	1.4pp	19%	3.8%	5.2%	1.4pp	36%
Central	32.0%	32.7%	0.7pp	2%	23.4%	23.6%	0.2pp	1%	15.1%	15.5%	0.4pp	3%
Western	25.6%	25.3%	-0.3pp	-1%	17.1%	17.2%	0.2pp	1%	10.2%	10.0%	-0.2pp	-2%
Panel b: Eastern region												
Beijing	19.0%	23.2%	4.3pp	23%	12.1%	16.2%	4.1pp	34%	7.0%	10.7%	3.7pp	53%
Fujian	38.9%	45.6%	6.7pp	17%	24.6%	32.5%	7.9pp	32%	14.1%	19.0%	4.9pp	35%
Guangdong	51.9%	55.5%	3.7pp	7%	37.5%	45.3%	7.8pp	21%	21.6%	26.3%	4.7pp	22%
Hainan	63.5%	63.4%	0.0pp	0%	47.1%	51.8%	4.7pp	10%	27.7%	31.5%	3.9pp	14%
Hebei	24.4%	25.1%	0.7pp	3%	17.0%	18.0%	1.0pp	6%	10.8%	12.3%	1.5pp	14%
Jiangsu	30.5%	29.7%	-0.8pp	-3%	22.5%	21.5%	-1.0pp	-4%	14.3%	13.7%	-0.6pp	-4%

Continued on next page

Table D.8: Regional Average Share of Time at Risk of Exposure to Moderate Heat Stress Thresholds for Children (ages 0-14), 1990 to 2020

	At least borderline thermal stress				At least moderate heat stress							
	⩾ UTCI 23° C				⩾ UTCI 26° C				⩾ UTCI 29° C			
	Share of time		Changes		Share of time		Changes		Share of time		Changes	
Location	1990	2020	Level	%	1990	2020	Level	%	1990	2020	Level	%
Shandong	26.7%	25.3%	-1.4pp	-5%	18.1%	18.2%	0.0pp	0%	11.4%	12.1%	0.7pp	6%
Shanghai	27.9%	29.7%	1.8pp	7%	19.7%	20.7%	1.0pp	5%	12.3%	11.3%	-1.0pp	-8%
Tianjin	23.5%	25.2%	1.7pp	7%	15.8%	17.8%	1.9pp	12%	9.7%	12.1%	2.3pp	24%
Zhejiang	33.4%	36.0%	2.6pp	8%	22.6%	26.5%	3.9pp	17%	13.6%	15.4%	1.8pp	13%
Panel c: Northeastern region												
Heilongjiang	10.2%	11.2%	1.0pp	9%	6.3%	7.3%	0.9pp	15%	2.9%	4.0%	1.1pp	38%
Jilin	11.1%	12.2%	1.1pp	10%	6.9%	8.5%	1.5pp	22%	3.4%	4.9%	1.5pp	45%
Liaoning	14.4%	15.8%	1.4pp	10%	9.1%	10.3%	1.3pp	14%	5.1%	6.2%	1.1pp	21%
Panel d: Central region												
Anhui	32.7%	32.3%	-0.4pp	-1%	25.2%	23.4%	-1.8pp	-7%	16.2%	15.5%	-0.7pp	-5%
Henan	29.6%	29.4%	-0.2pp	-1%	21.5%	21.1%	-0.4pp	-2%	13.9%	14.5%	0.6pp	4%
Hubei	33.3%	33.9%	0.6pp	2%	25.1%	24.2%	-0.9pp	-3%	16.7%	15.4%	-1.3pp	-8%
Hunan	36.2%	37.6%	1.4pp	4%	25.7%	26.8%	1.1pp	4%	16.5%	17.1%	0.5pp	3%
Jiangxi	38.8%	41.8%	3.0pp	8%	28.1%	31.7%	3.6pp	13%	17.9%	20.9%	3.1pp	17%
Shanxi	16.1%	16.6%	0.5pp	3%	10.6%	11.1%	0.6pp	5%	6.0%	6.6%	0.5pp	9%
Panel e: Western region												
Gansu	11.1%	10.7%	-0.4pp	-3%	6.6%	6.4%	-0.2pp	-3%	3.0%	2.9%	0.0pp	-1%
Guangxi	47.5%	49.2%	1.7pp	4%	33.3%	36.8%	3.4pp	10%	20.2%	21.4%	1.2pp	6%
Guizhou	19.5%	19.4%	-0.1pp	0%	12.2%	11.6%	-0.6pp	-5%	7.0%	6.1%	-0.9pp	-13%
Neimenggu	9.9%	12.0%	2.1pp	21%	6.0%	8.2%	2.2pp	36%	2.9%	4.7%	1.8pp	62%
Ningxia	12.9%	14.1%	1.1pp	9%	8.8%	9.6%	0.8pp	10%	5.0%	5.7%	0.7pp	13%
Qinghai	4.9%	3.8%	-1.1pp	-23%	1.4%	1.0%	-0.4pp	-30%	0.1%	0.0%	-0.1pp	-71%
Shaanxi	19.5%	19.3%	-0.2pp	-1%	13.3%	13.1%	-0.3pp	-2%	8.6%	8.2%	-0.3pp	-4%
Sichuan	28.5%	29.4%	0.8pp	3%	19.3%	19.7%	0.4pp	2%	12.5%	12.2%	-0.3pp	-3%
Xinjiang	16.3%	18.0%	1.6pp	10%	11.4%	13.1%	1.7pp	14%	7.4%	8.8%	1.4pp	18%
Xizang	1.3%	1.4%	0.1pp	5%	0.1%	0.1%	0.0pp	-32%	0.0%	0.0%	0.0pp	159%
Yunnan	19.2%	21.0%	1.8pp	9%	11.0%	12.3%	1.3pp	12%	4.6%	5.3%	0.8pp	17%

Note: We present similar statistics as in Table D.1, but now compute exposures separately for four economic regions and provincial-level administrative units in China. Columns (cols) 4–6 and 7–9 focus on at least Moderate UTCI heat exposure at ⩾ 26 °C and ⩾ 29 °C, respectively. Cols 1–3 provide UTCI heat exposure at ⩾ 23 °C, where UTCI 23 °C is a temperature level that is just below the threshold (25 °C) for Moderate heat stress. Cols 1 and 2, 5 and 6, and 9 and 10 show the annual average share of time at risk of exposure to heat stress thresholds (UTCI temperatures at ⩾ z °C) for children in China (ages 0–14). Cols 3 and 4, 7 and 8, and 11 and 12 show 1990 to 2020 changes in percentage points (level) or percentage (%) of the average shares of time exposed to heat. Cells are empty for percentage changes when the denominator is equal to zero. We consider all 24 hours and 12 months.

E Connecting Additional Analyses to Literature

Comparing our additional analyses to the existing literature that considers deeper aspects of heat exposure: amongst the regions of China; across different months/seasons; contrasting day and night-time exposure; and on the provincial level, we find a decreasing amount of research dedicated to each perspective.

E.1 Seasonal & Regional Analyses

Regional and seasonal focus on heat exposure is prevalent in the literature, especially focusing on discreet heat events, with many studies addressing both elements. Our results showcase the increased intensity of heat exposure primarily occurring amongst east and northeast China with the latter having sizeable increases due to the warming up of its especially cold climate. Seasonally, we also found that winters across China are facing large changes since 1990. Existing literature broadly supports both of our observations.

Multiple longitudinal studies use summer weather station data across decades to track temperature change throughout China's regions. While these studies are limited in their lack of consideration of dynamic population counts, they still support our analysis in finding consistent if not rising heat stress in the summer along with a drop in Cold Stress and No Heat Stress days, particularly in northeastern China (Wu et al. 2017; Yan et al. 2019; Zhou et al. 2016). Other supporting studies find an increase in heatwave days and frequency across China but with historically distinct rises and falls in the south and north (Feng et al. 2023; Hu, Huang, and Qu 2017; Luo and Lau 2019; You et al. 2017); with distinct risk for the most population-dense region of the southeast (Feng et al. 2023).

The regional and seasonally-specific heat exposure literature is in line with our observations: much of the increase of heat stress can be attributed to large changes in traditionally colder regions and seasons, along with heat intensification of the already hot and populous southeastern regions of China.

E.2 Day/Night-time Exposure & Provincial Exposure

Whereas we find many additional studies performing deeper analyses on seasonal and regional variations in heat exposure in China, much less research exists for day and night, and especially province-specific analysis. To briefly reiterate, we find that daytime hours at Strong

and Very Strong heat stress are consistent with all annual hours' change in exposure, while at lower stress thresholds, daytime changes in exposure are lower than all hours' change thus implicitly indicating the increase in nightly heat stress. Provincially, we find large changes in strong heat stress in eastern provinces with variation between provinces on the lower end likely due to low population density in the colder northeast and warmer west, and high exposure change in the most populous provinces in the east. The literature that does exist supports our analyses. Wang and Sun (2021) use wet bulb global temperature to analyze changes in interdecade extreme summer heat indices in China. They find an increase in warm days and nights since 1961 and a pronounced decrease in cold days and nights in northwestern China.

Additional support from Sun et al. (2024) also demonstrates the importance of time and population variation on the inter-provincial level when it comes to heat exposure by looking into Beijing and dynamic population change throughout time during the day over a 5-day heatwave event in June and July 2019. Sun et al. (2024) visualizes increased temperature and population-weighted temperature during the day as people move through Beijing's urban and suburban geographies and thus are exposed to more or less heat stress. We note that Sun et al. (2024) is one of the few studies to so closely consider heat exposure on the province level, albeit on a singular provincial municipality. While much research does exist mapping heat patterns across China, less so focuses on categorizing that exposure by administrative borders. Isolated studies such as this one and the previously cited Dong, Tao, and Zhang (2023) on historic heat exposure of the Xinjiang province are still inherently limited due to a lack of consideration of multiple provinces' heat exposure at once.

In sum, our additional analyses support the robustness of our study. We continue to emphasize that the analyses performed in the literature lack a thorough consideration of temperature and population distributions, let alone child-specific population considerations.

E.3 Additional info on papers